Theses and Dissertations   1. Thesis and Dissertation Collection, all items

1973-03

A computer technique for near-field analysis of ultrasonic transducer.

Griggs, Carlton Albert.

Monterey, California. Naval Postgraduate School
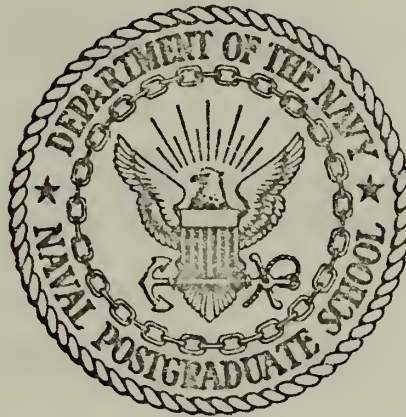
http://hdl.handle.net/10945/16536

A COMPUTER TECHNIQUE FOR NEAR-FIELD
ANALYSIS OF AN ULTRASONIC TRANSDUCER

Carlton Albert Griggs

NAVAL POSTGRADUATE SCHOOL
Monterey, California

THESIS

A COMPUTER TECHNIQUE FOR NEAR-FIELD
ANALYSIS OF AN ULTRASONIC TRANSDUCER

BY

Carlton Albert Griggs

Thesis Advisor: J. P. Powers

March 1973   T153736

A Computer Technique for Near-Field
Analysis of an Ultrasonic Transducer

by

Carlton Albert Griggs
Lieutenant Commander, United States Navy
B.S., United States Naval Academy, 1964

Submitted in partial fulfillment of the
requirements for the degree of

MASTER OF SCIENCE IN ENGINEERING ACOUSTICS

from the
NAVAL POSTGRADUATE SCHOOL
March 1973

2

ABSTRACT

A computer technique for obtaining near-field cross-section views of an ultrasonic field is presented. The technique is applied to ultrasonic transducer radiation patterns with sample contour drawings of several cross-sections. A spatial frequency spectrum formulation of diffraction theory is chosen for the computations which are performed with the aid of a fast Fourier transform routine.

By experimentation an actual ultrasonic field was generated using a quartz transducer and the field was measured in a cross-sectional plane. A computer generated drawing of the measured data is compared to the drawing of a computer generated prediction of the field at the same plane.

The computer model is applied to an array of transducers to investigate the resulting ultrasonic field, as a preliminary use of the technique for array design.

TABLE OF CONTENTS

I. INTRODUCTION

The work in this study was in connection with ultrasonic imaging systems studies at the Naval Postgraduate School. The study undertaken here was generated by the need for a large-area ultrasonic field as delineated in Ref. 1. One possible way of producing a large planar wavefront is by synthesis of a large array from smaller transducers. Due to the large distribution of variables involved in designing a near-field array, a fast and practical means of producing near-field information was first required. A large body of literature is available for simple apertures in the near-field and C. M. McKinney et al recount the history of this research very concisely in Ref. 2. Exact expressions of the near-field are developed through essentially the same methods. They all involve finding a solution to the wave equation which satisfies certain assumed boundary conditions. The resulting integral equations are unwieldy even for the simplest aperture shapes because the field cannot be expressed in terms of elementary functions. The ability to project planes of data in the near-field to other planes within the near-field is therefore a most valuable facility in terms of making maximum use of both theoretical and empirical data available for design purposes. Developing a model to make these plane-to-plane projections was the major task undertaken in this study. A starting point for planning

4

the work was a study of the imaging technique reported by A. L. Boyer et al [Ref. 3].

As a test of the model developed, the distribution of a square aperture's diffraction pattern was predicted at various planes throughout the field. The model was then used to predict the field of a quartz transducer. The actual field distribution of the quartz transducer modeled on the computer was measured after setting up the necessary experimental apparatus. A piezoelectric probe attached to a mechanical scan system was used to collect the data. A preliminary use of the data was the comparison of a predicted and a measured field distribution in a plane within the near-field of the source. The data taken in this experiment should be useful for future work in this and related areas of imaging system studies.

Time allowed the use of the computer model to make predictions of the near-field distribution of a transducer array. However, the use of the computer model for array design was done only in a preliminary manner by examining an assumed array which was relatively simple to model. This allowed the method of design to be evaluated although a design problem itself could not be accomplished within the time alloted for this work.

II. <u>THEORY</u>

A. THE GENERAL SCHEME

The purpose of this section is to present some of the fundamental concepts of an approach taken for computer modeling of the near-field of a transducer. It is not intended as a rigorous proof in the foundations of spatial frequency spectrum theory [Ref. 4], but rather a justification of the computer scheme used in this study. The overall scheme is one which allows the prediction of a complex near-field distribution in a plane on the basis of a known complex field distribution in any other plane perpendicular to the direction of propagation. Based on the assumption that the planar distribution of a sound field at the transducer takes on the geometry and motion of the transducer itself, predictions of the sound field distribution at various planes throughout the near-field were made with the computer model. Figure 2-1 is a schematic which is helpful in organizing the operations involved in the following subsections. The subsections contain an explanation of the symbols which appear in Fig. 2-1.

B. THE SPATIAL FREQUENCY SPECTRUM

Let an isolated sound source be contained entirely within a source plane as shown below in Fig. 2-2.
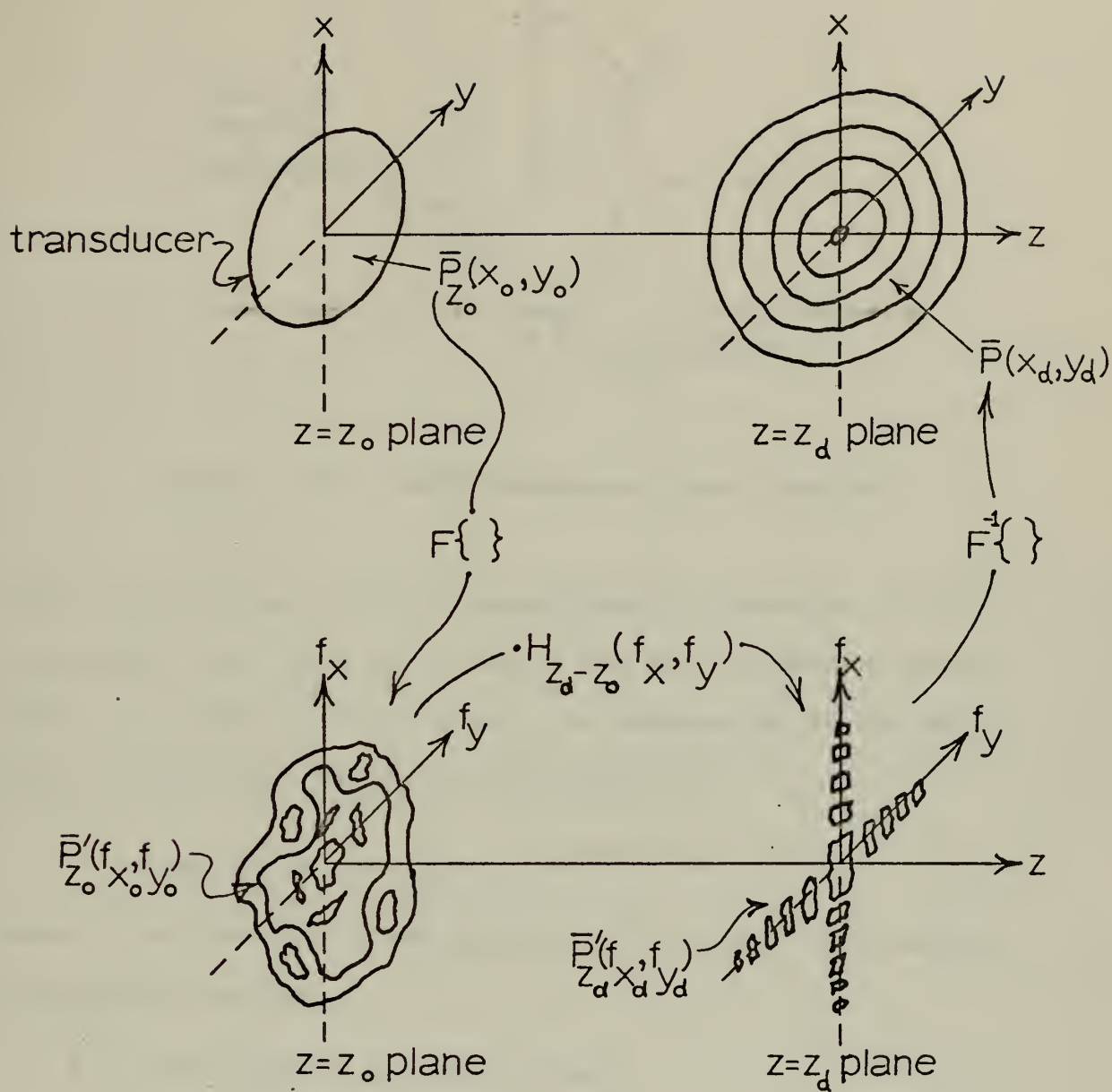
Figure 2-1. The Propagation Model Sequence of Operations.
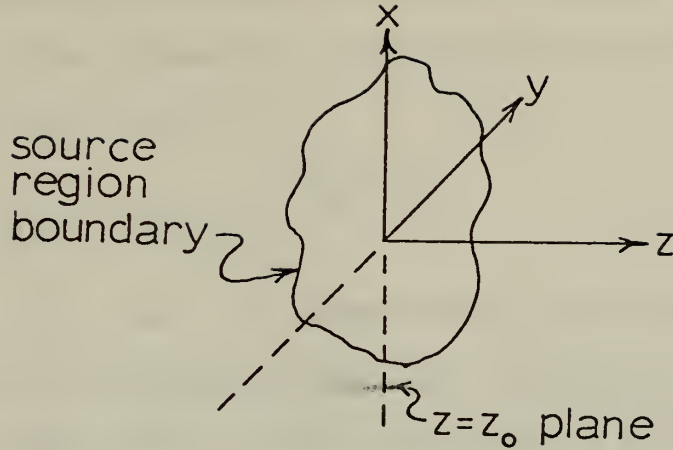
Figure 2-2. Two-dimensional Sound Source.

Given that the source is a monochromatic pressure field in free space, and that x, y, and z are the cartesian coordinates of a typical field point, an expression of the pressure distribution in the source plane is

$$\bar{P}(x,y,z_o t) = P(x,y,z_o) \ e^{j\phi(x,y,z_o)} \ e^{-j\omega t} \qquad (2.1)$$

where t is time and ω the angular frequency. Also defined are the following:

   $\bar{P}$ ≡ the complex pressure phasor

   P ≡ the peak pressure amplitude

   ϕ ≡ the phase of the complex phasor

   z_o ≡ the source plane position on the z axis

For convenience an abbreviation in notion is used hereafter such that

$$\bar{P}_z(x,y,t) = \bar{P}(x,y,z,t) \qquad (2.2)$$

8

where the subscript denotes the plane located at z. Assuming harmonic time dependence the expression for complex pressure is simplified to

$$\bar{P}_z(x,y) = P_z(x,y) \ e^{j\phi_z(x,y)} \tag{2.3}$$

In viewing $\bar{P}_z(x,y)$ as a two dimensional distribution for a given z plane, the decomposition of the distribution into a spectrum of plane waves proves convenient. A decomposition of the distribution can be formed by use of a two-dimensional Fourier transform as given by Goodman [Ref. 5].

$$\bar{P}_z'(f_x,f_y) = \int\!\!\!\int_{-\infty}^{\infty} \bar{P}_z(x,y)\exp[-j2\pi(f_xx+f_yy)] \ dxdy \tag{2.4}$$

Goodman further shows that the original distribution $\bar{P}_z(x,y)$ can now be written in terms of its spatial frequency spectrum by use of the inverse Fourier transform as shown by

$$\bar{P}_z(x,y) = \int\!\!\!\int_{-\infty}^{\infty} \bar{P}_z'(f_x,f_y) \ \exp[j2\pi(f_xx+f_yy)] \ df_xdf_y \tag{2.5}$$

The spatial frequencies, f_x and f_y, can be related to a unique orientation of the propagation vector, $\vec{k}$, for a given plane wave in 3-dimensional space. Where k, the propagation constant, is given by $k = 2\pi/\lambda = 2\pi f/c$, and f is the spatial frequency of a propagating plane wave in the direction of propagation; the vector, $\vec{k}$, has magnitude, k, in the direction of an outward normal from the planewave wavefront. Let the vector, $\vec{k}$, be separated into its components in the coordinate system by forming its dot product with a radius vector, $\vec{r}$, such that

$$\vec{k} \cdot \vec{r} = k_x x + k_y y + k_z z = 2\pi (f_x x + f_y y + f_z z) \qquad (2.6)$$

Eq. 2.6 can be written in terms of the x-y plane spatial frequencies alone by making the following substitution:

$$f_z = \sqrt{\frac{1}{\lambda^2} - f_x^2 - f_y^2}$$

In the form given in Eq. 2.5, $\bar{P}_z(x,y)$ expresses the distribution of sound pressure over the observed plane, z, as a superposition of plane waves and evanescent waves. Plane waves are implied when $f_x^2 + f_y^2 \leq \frac{1}{\lambda^2}$ and evanescent waves are implied when $f_x^2 + f_y^2 > \frac{1}{\lambda^2}$ [Ref. 6].

C. PROPAGATION OF THE SPATIAL FREQUENCY SPECTRUM

The propagating waveform must satisfy the homogeneous wave equation in 3-dimensional space. $\bar{P}_z(x,y)$ in the frequency spectrum formulation as given in Eq. 2.5 is required to satisfy the Helmholtz equation

$$\nabla^2 \bar{P}_z + k^2 \bar{P}_z = 0 \qquad (2.7)$$

The solution of the Helmholtz equation leads to a second order differential equation in the variable z. Its solution is given in Ref. 5 as

$$\bar{P}_z(x,y) = \int\!\!\int_{-\infty}^{\infty} \bar{P}_z'(f_x, f_y) \exp\left[j2\pi\sqrt{\frac{1}{\lambda^2} - f_x^2 - f_y^2}\; z\right] \exp\left[j2\pi(f_x x + f_y y)\right] df_x df_y \qquad (2.8)$$

Comparing Eq. 2.5 and Eq. 2.8 it is apparent that Eq. 2.8 can be considered the two-dimensional Fourier transform of that portion of the expression under the integral given by

$$\bar{P}_z'(f_x, f_y) = \exp\left[j2\pi z \sqrt{\frac{1}{\lambda^2} - f_x^2 - f_y^2}\right]$$

This expression suggests that propagation could be modeled in the Fourier transform domain using as a transfer function

$$H(f_x, f_y) = \exp\left[j2\pi z \sqrt{\frac{1}{\lambda^2} - f_x^2 - f_y^2}\right] \qquad (2.9)$$

by merely taking the inverse transform of $P_z'(f_x, f_y) \cdot H(f_x, f_y)$ where z in Eq. 2.9 is taken as the distance between the reference plane and the observed plane.

D.   TWO-DIMENSIONAL LINEAR SYSTEM

It remains to be shown that the propagation from one plane to another can be considered an overall linear system to justify the transfer function approach to modeling.   In a linear system the total response is equal to the combination of elementary responses, or mathematically stated the superposition property holds [Ref. 7].   In order to demonstrate this property of frequency spectrum propagation, it is convenient to express the waveform at an observed plane $z = z_d$ in terms of the waveform at a reference plane, $z = z_o$.

To formulate a wave distribution at the $z = z_o$ plane as shown in Fig. 2-3, a substitution of f_z into Eq. 2.8 and a regrouping of that expression leads to a planar distribution given by

$$\bar{P}_{z_o}(x_o, y_o) = \int\!\!\int_{-\infty}^{\infty} \bar{P}_{z_o}'(f_x, f_y) \exp[j2\pi(f_x x_o + f_y y_o + f_z z_o)]\, df_x df_y \qquad (2.10)$$

11
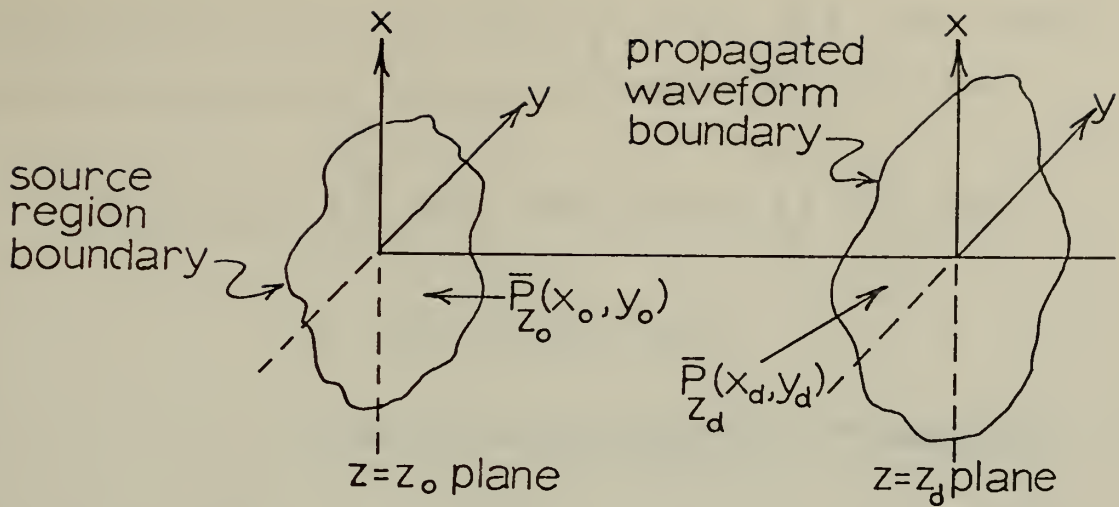
Figure 2-3. Boundaries and Distributions of a Propagated Wave Distribution at Two Planes.

When the Fourier transform is denoted by $F\{\ \}$ and the inverse Fourier transform by $F^{-1}\{\ \}$, Eq. 2.10 becomes

$$\bar{P}_{z_o}(x_o, y_o) = F^{-1}\left\{\bar{P}'_{z_o}(f_x f_y)\ e^{j2\pi f_z z_o}\right\} \tag{2.11}$$

Taking the Fourier transform of Eq. 2.11 and reordering the equation gives

$$\bar{P}'_{z_o}(f_x f_y)\ \exp\left[j2\pi f_z z_o\right] = F\left\{\bar{P}_{z_o}(x_o, y_o)\right\} \tag{2.12}$$

which can be equated to solve for $\bar{P}'_{z_o}(f_x, f_y)$ as given by

$$P'_{z_o}(f_x, f_y) = \exp[-j2\pi f_z z_o]\ \int\!\!\int_{-\infty}^{\infty} \bar{P}_{z_o}(x_o, y_o)$$

$$x\ \exp[-j2\pi(f_x x_o + f_y y_o)]\ dxdy \tag{2.13}$$

At the plane $z = z_d$ write the expression for $\bar{P}_{z_d}(x_d, y_d)$ by

12

substituting Eq. 2.13 for $P_z'(f_x, f_y)$ in Eq. 2.8. The resulting expression for $\bar{P}_{z_d}(x_d, y_d)$ in terms of $\bar{P}_{z_o}(x, y)$ is:

$$\bar{P}_{z_d}(x_d y_d) = \int\!\!\int_{-\infty}^{\infty} \exp[-j2\pi f_z(z_d - z_o) \int\!\!\int_{-\infty}^{\infty} \bar{P}_{z_o}(x_o y_o)$$

$$x \, \exp[-j2\pi(f_x x_o + f_y y_o)]$$

$$x \, \exp[j2\pi(f_x x_d + f_y y_d + f_z z_d)] dx_o dy_o df_x df_y \quad (2.14)$$

By interchanging the order of integration of this equation and by making the simplification in notation that

$$K_{do}(x_d - x_o, y_d - y_o) = \int\!\!\int_{-\infty}^{\infty} \exp\left\{j2\pi[f_x(x_d - x_o)\right.$$

$$\left. + f_y(y_d - y_o) + f_z(z_d - z_o)]\right\} df_x df_y \quad (2.15)$$

the final form of the expression of $\bar{P}_{z_d}$ at the $z = z_d$ plane in terms of at the $z = z_o$ plane can be expressed as

$$\bar{P}_{z_d}(x_d y_d) = \int\!\!\int_{-\infty}^{\infty} \bar{P}_{z_o}(x_o y_o) K_{do}(x_d - x_o, y_d - y_o) dx_d dy_d \quad (2.16)$$

Systems whose output can be expressed in this form as a function of the input are recognized to be linear systems [Ref. 8]. Thus the wave distribution at the $z = z_d$ plane is given in terms of the distribution at the $z = z_o$ plane by Eq. 2.16 when the system transfer function is given by Eq. 2.15.

In the computer model developed for Eq. 2.9 evanescent waves were neglected and the transfer function was therefore

13

bandlimited to those frequencies within a circle of radius
$1/\lambda$. This at first appears to limit the class of pressure
distributions which can be considered to those which have
bandlimited spatial frequency distributions. However, evan-
escent waves decay exponentially with increased distance in
the z-direction, and their effect on the field is insignifi-
cant in planes greater than a few wavelengths from the source.
The region of the field where the evanescent waves have a
significant effect on the pressure distribution is sometimes
called the very-near-field. Acoustic imaging systems
usually reconstruct the image from the pressure distribution.
Reconstruction of an image requires that the evanescent
waves be accounted for in the superposition integral of the
type given in Eq. 2.16. Since the evanescent waves do not
propagate, the near-field and far-field distributions are
independent of their presence. Neglecting the evanescent
waves, therefore, did not restrict the ability to make
plane-to-plane predictions in the near-field as long as the
reference distribution was measured at a distance greater
than a few wavelengths from the transducer. Expressing
Eq. 2.9 in a more appropriate form for the model which
neglects the evanescent waves

$$H(f_x, f_y) = \begin{cases} \exp j2\pi z \sqrt{\dfrac{1}{\lambda^2} - f_x^2 - f_y^2} & : \quad \text{if } f_x^2 + f_y^2 < \dfrac{1}{\lambda^2} \\ 0 & : \quad \text{otherwise} \end{cases} \qquad (2.17)$$

14

E. THE DISCRETE FOURIER TRANSFORM

Let X and Y be the sample intervals in the spatial x and y coordinate directions respectively. Let Ω_x and Ω_y be the corresponding sample intervals in the spatial frequency plane. The discrete Fourier transform (DFT) over a region N and M samples long in the x and y directions respectively is defined as

$$F(k\Omega_x, \ell\Omega_y) = \sum_{n=0}^{N-1} \sum_{m=0}^{M-1} f(nX, mY)$$

$$x \; \exp[-j(nXk\Omega_x + mY\ell\Omega_y)] \qquad (2.18)$$

where $\quad 0 \le k \le N-1 \quad$ and $\quad 0 \le \ell \le M-1$

and

$$\Omega_x = \frac{2\pi}{NX} \qquad \Omega_y = \frac{2\pi}{MY}$$

These equations are in the form of those which were implemented with the fast Fourier transform (FFT) algorithm called "FOUR2" [Ref. 9]. The Fortran statements of these programs are included in Appendix A. The FOUR2 subroutine was used to perform the transformation to and from the spatial frequency spectrum domain.

F. PROPAGATION BY TRANSFER FUNCTION

When Eq. 2.17 is placed into a discrete format as follows:

$$H(k\Omega_x, \ell\Omega_y) = \begin{cases} \exp\left[j2\pi z \sqrt{\dfrac{1}{\lambda^2} - (k\Omega_x)^2 - (\ell\Omega_y)^2} \right] : \\ \qquad\qquad (k\Omega_x)^2 + (\ell\Omega_y)^2 < \dfrac{1}{\lambda^2} \\ \\ 0 \quad : \quad \text{elsewhere} \end{cases} \qquad (2.19)$$

or more simply written

$$
H_{k,\ell} = \begin{cases} \exp[j2\pi z \sqrt{\dfrac{1}{\lambda^2} - \Omega^2_{xy}(k^2+\ell^2)}] & \text{if} \quad (k^2+\ell^2)(\lambda\Omega_{xy})^2 < 1 \\ \\ 0 & \text{if} \quad (k^2+\ell^2)(\lambda\Omega_{xy})^2 \geq 1 \end{cases} \tag{2.20}
$$

The propagation algorithm as given in Appendix A was used to perform the multiplication of the transformed input data by the transfer function (Eq. 2.20).

G. ANALOG-TO-DIGITAL CONVERSION

When predicted patterns of the waveform at various planes were calculated on the basis of their aperture function, the data was arranged in the shape of the aperture with uniform amplitude and phase samples everywhere within the aperture. However, the analog data collected in the experimental portion of this analysis had to be converted to sampled data before being utilized in the propagation program. The analog-to-digital, A/D, conversion process was done by the simultaneous utilization of an XDS 9300 digital computer and a COMCOR Ci 5000 analog computer. A lengthy description of the facilities and equipment used, the A/D conversion process, and the seven-to-nine track conversion was a necessary step in making the digital data of the XDS 9300 computer compatable with the IBM 360/67 computer requirements.

H. AN INTERPOLATION OF DIGITAL DATA DISPLAY

The subroutine CONTUR [Ref. 11] included as part of Appendix B, was used to produce separate analog displays of

the amplitude and phase at a desired plane. In this routine
a pseudo three dimensional effect is presented by contour
lines. Coarse analysis of an entire cross-section of the
field can be performed from contour drawings.

I. FLOWCHART OF STEPS IN COMPUTER OPERATIONS

A flowchart of the computer operations in the order
performed and a description of the equipment used in con-
junction with each step is given in Fig. 2-4.

J. INHERENT ADVANTAGES AND DISADVANTAGES OF THE DFT AND FFT

Since Cooley and Tukey first reported the algorithm
which they developed for the FFT [Ref. 12], the amount of
literature which has been published on applications of this
technique of computation and its advantages and disadvantages
would fill volumes. Much insight into the FFT technique can
be gained from Refs. 13-15. Much less has been written
about applying this technique for processing of data in the
two dimensional spatial frequency domain. Reference 13 was
the most germane discussion found for this study. It
discusses the problems commonly called leakage and aliasing
in articles which treat time-frequency analysis problems
[Ref. 14].

The problem of leakage can sometimes work as an advan-
tage in spatial frequency analysis. Leakage is an approxi-
mation error which arises from a finite record length
representation of an infinite length record. Its affect on
the desired spectrum is equivalent to an undesired convolu-
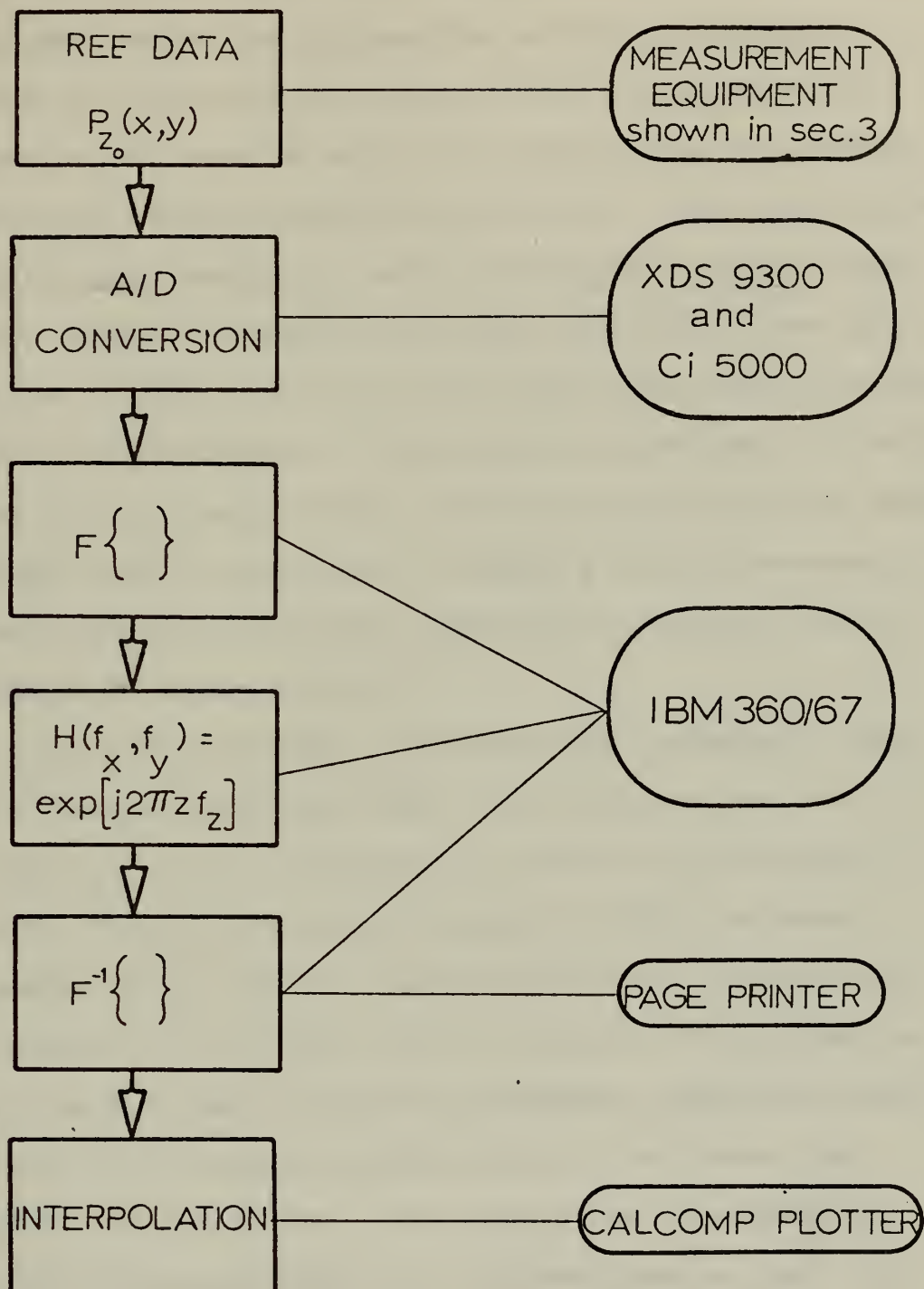tion of a data window with the true frequency spectrum. The

Figure 2-4.   Flowchart of Computer Operations for
              Propagation Modeling.

window occurs because of the geometry of the termination of the record. In this study a transducer array was in reality a truncated source and propagation of the data window resulted in a diffraction effect of the window geometry. Diffraction was modeled using this effect when the square shape of the sampled lattice was suitable. When the square window did not adequately model the geometry desired, the simplest method of modeling the edge diffraction was found to be one of leaving a border of zeroed data around the data field to be transformed. This method reduced the diffraction effects of the square sample lattice at the cost of a greatly increased memory requirement to model a given transducer. A discussion of the truncation approach to handling various geometries is given in Ref. 17.

Aliasing is a problem associated with modeling a continuous Fourier transform (CFT) by a discrete Fourier transform (DFT). It is, therefore, an inherent disadvantage of the DFT. The term "aliasing" refers to high frequency components of the spatial function which are incorrectly represented due to widely spaced sampling. The effect is worse than the loss of the high frequency components since it results in erroneous coefficients in the lower frequencies of the spectrum. The effect can be avoided by sampling the waveform with the optimum spacing [Ref. 18]. The sample spacing when determined by the two-dimensional sample theorem frequently led to excessive numbers of samples necessary to represent a given transducer. Since

19

computations were computer memory limited, a corresponding limit was placed on the total number of samples available to represent a cross-section of the field. A compromise in choosing sample spacing and border width around the representative data was necessary.

The disadvantages of the FFT associated with modeling the diffraction equations were insignificant when compared to those of the DFT. That is to say that the errors in modeling of the diffraction came from making the transition from a CFT to a DFT not in the FFT algorithm itself. The worth of the algorithm is measured in terms of speed, efficiency, memory required and round-off error. Of these, the requirement for a large memory is the only significant disadvantage. Although this study was seriously limited by the computer memory available, there are means to circumvent this problem by using more computation time. This is a matter of optimizing the algorithm to the particular region of the propagating waveform that is of interest. For this work, three versions of the algorithm listed in Appendix B were required. The subroutine "FOUR2" makes very effective use of time in performing the calculations of the FFT, however, the total number of sample points (record length) must be a power of 2. Reference 19 gives an algorithm which can transform many different record lengths at a moderate cost in increased computation time. Implementation of this "mixed radix" form of algorithm is strongly recommended for future studies of transducer sound field analysis.

III.   EXPERIMENTAL INVESTIGATION

Experimental data was taken for two primary reasons. First was the desire for a means of evaluating the computer predictions. Second was the desire for actual data vice the assumed data at the face of the transducer as mentioned in Section II to evaluate the assumptions of the model itself. A mechanical scan probing system was constructed to measure the complex sound field of a transducer to be described.

A.   THE WATER TANK

The water tank used in this experiment was constructed of plywood and lined with a one inch thickness of poly-styrene. The inner dimensions provided for a column of water 4½ inches deep, 4 inches wide and 45 inches long. A cross section of this column was not large enough to con-sider the propagating wave entirely unbounded. However, it was found by experiment that the difference in nearby rigid and nearby release surface measurements were not significant until the hydrophone probe was within approximately ten wavelengths of the boundary. All data was taken with this consideration limiting the field of data. The length of the tank used was considered adequate to approximate an infinite medium at the frequency used. The tank was lined with poly-styrene which was a composition of pliable thermoplastic with a high absorption coefficient. Its impedance is very close to that of air for which $\rho_a C_a$ = 415 rayls.

B. THE HYDROPHONE PROBE

In design of the hydrophone (Fig. 3-7a), an attempt was made to minimize reflections affecting the free field measurement. The active face of the probe is 0.04 inches in diameter (0.83 wavelengths @ 1012 kHz). A thickness vibrator type receiver of PZT-5 ceramic composition is produced by Valpy-Fisher. .It is encapsuled with a bronze impedance matched backing and provided with a shielded electrical connector by the manufacturer. This type probe was mounted for use as a hydrophone in a plexiglass holder and coated with neopreme.

C. THE TRANSDUCER

The source transducer is shown in Fig. 3-1b. The crystal shown is a 2 inch by 2 inch square transducer of X-cut quartz. This transducer is designed as a thickness vibrator polished for a fundamental frequency of 1 MHz with good overtone opera-tion characteristics. The peak output signal from the probe was obtained when driving the transducer at 1012 kHz. Con-sequently that frequency was chosen for all data collected. The small offset from the transducer's fundamental resonance was necessary due to the mis-match in resonant frequencies of transducer and probe.

D. THE MECHANICAL SCAN EQUIPMENT

The mechanical scan equipment mounted above the measure-ment tank is shown in Fig. 3-2. The scanning system became an important concern in fabricating the measurement apparatus
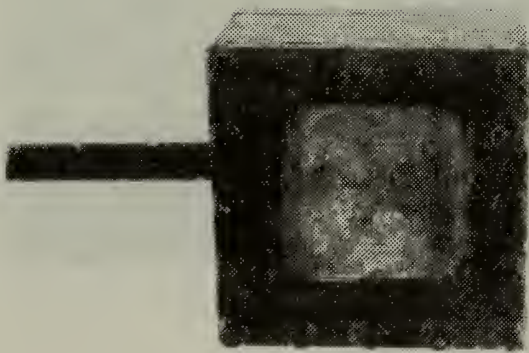
(a)
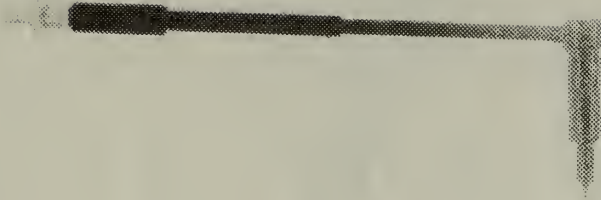
(b)

Figure 3-1.   (a)   The 2 Inch Square Quartz Crystal and Transducer Mounting.
              (b)   Valpy-Fisher PZT-5 Probe and Hydrophone Mounting.

Figure 3-2. Measurement Tank and Mechanical Scan System.

because three rigid system requirements depended upon the scan mechanism. The first was the requirement to insure that phase information be recorded accurately to within ±10 degrees. This meant that the recording plane would have to be flat to within 0.04 millimeters at the frequency used of 1012 kHz. A similar precaution was taken by Boyer et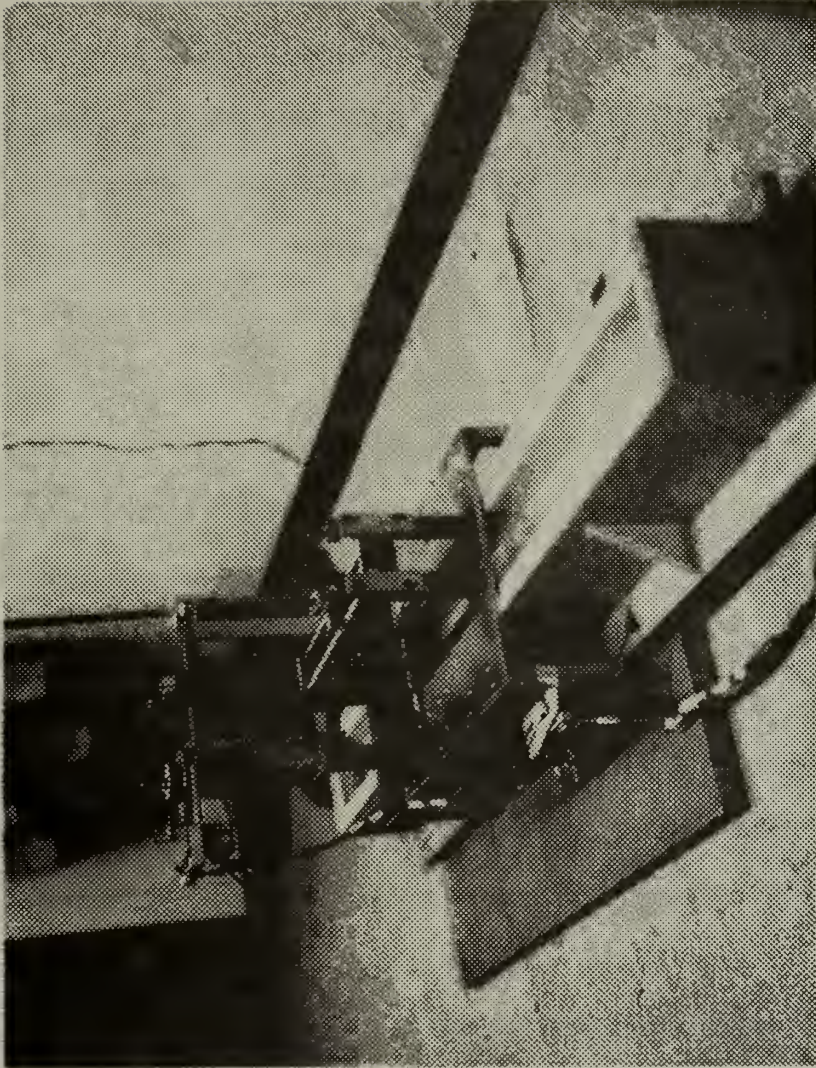 al as noted in Ref. 3. The second requirement was that the scan system be equipped to measure position accurately to within a small fraction of a wavelength. Still a third requirement was that it provide a means of taking data rapidly enough to collect a large quantity of data in a reasonable length of time. The heart of the scan system was a mechanical scan unit taken from a disassembled fire control computer. This unit, driven by a variable speed motor, positioned the probe horizontally across the width of the tank. A manually operated slide assembly positioned the probe in the vertical dimension to vary its depth. The coordinate position of the probe within the cross-sectional plane was calculated by the advance per turn of the threads on the positioning mechanisms. The number of turns was recorded by hand from a mechanical counter in the vertical, and by a potentiometer in the horizontal direction. Analog records were taken for each depth as the motor driven assembly scanned the width of the tank. Uniform depth increments were used between records so that ultimately a square matrix of equally spaced data points would result. The assembled system produced data which shows a phase variation across the face of the transducer of 20

degrees peak to peak. The phase information recorded in
Fig. 3-3 was taken with the probe moving horizontally across
the width of the transducer 9.1 wavelengths in front of it,
at a point midway between the upper and lower edges of the
transducer. There is an overall shift in the mean phase
from the left edge to right edge of the transducer of
approximately 30 degrees. This indicates a misalignment of
the transducer and recording planes by 0.12 millimeters
maximum. Phase records were used in this manner to align
the transducer to the recording plane in both the horizontal
and vertical aspect. The maximum deviation in phase about
the mean was ±10 degrees when taken directly in front of the
transducer. On the basis of this and similar records it was
estimated that phase measurements were accurate to within
±10 degrees at the frequency used of 1012 kHz. Turns of the
scan positioning mechanisms were recorded accurately to
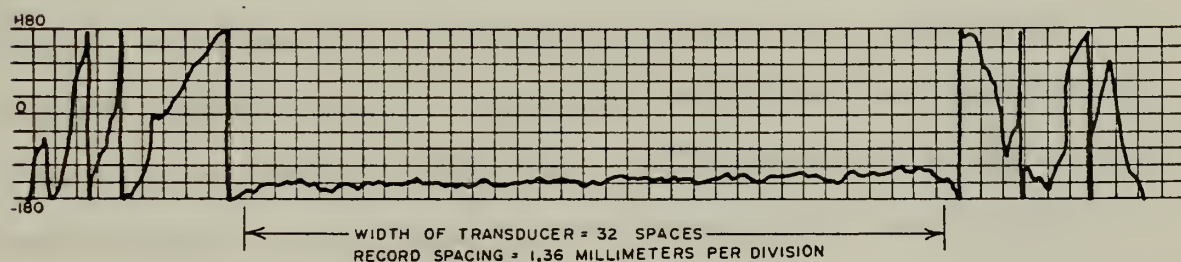within 1/36 of a turn with a resultant position accuracy of

WIDTH OF TRANSDUCER = 32 SPACES
RECORD SPACING = 1.36 MILLIMETERS PER DIVISION

Figure 3-3. Phase Variation across the Face of a Quartz
Transducer Radiating at 1012 kHz.

26

approximately 1/50 of a wavelength. The sample spacing was
9/10 of a wavelength at uniformly spaced intervals.

E. ELECTRONIC MEASURING EQUIPMENT

The general layout of electronic measurement equipment
is shown in Fig. 3-4 and a photograph of the physical layout
is given in Fig. 3-5. The electronic equipment layout was
an assembly of standard pieces of equipment. A
general description and specification summary is given
in Appendix B for the major components.

F. EXPERIMENTAL PROCEDURE

It was pertinent to the data reduction process that the
diameter of the hydrophone face was less than the sample
spacing, thus avoiding overlapping of the samples. Had
imaging been the desired use of the data collected, it would
have been ideal to sample the field at half-wavelength
intervals. The scanning system described in this experiment
could have been used for imaging if a more complex data
reduction process were used [Ref. 3]. The distance between
the transducer and the recording plane was adjusted by
moving the transducer which was mounted on a traveling
holder. Separation of transducer and probe was measured by
a scale graduated in 1/64 inch. If time had allowed repeated
experiments of this type, a mechanically driven threaded
shaft and traveler system would have been used for convenience
in observing ultrasonic wave behavior in the direction of
propagation.
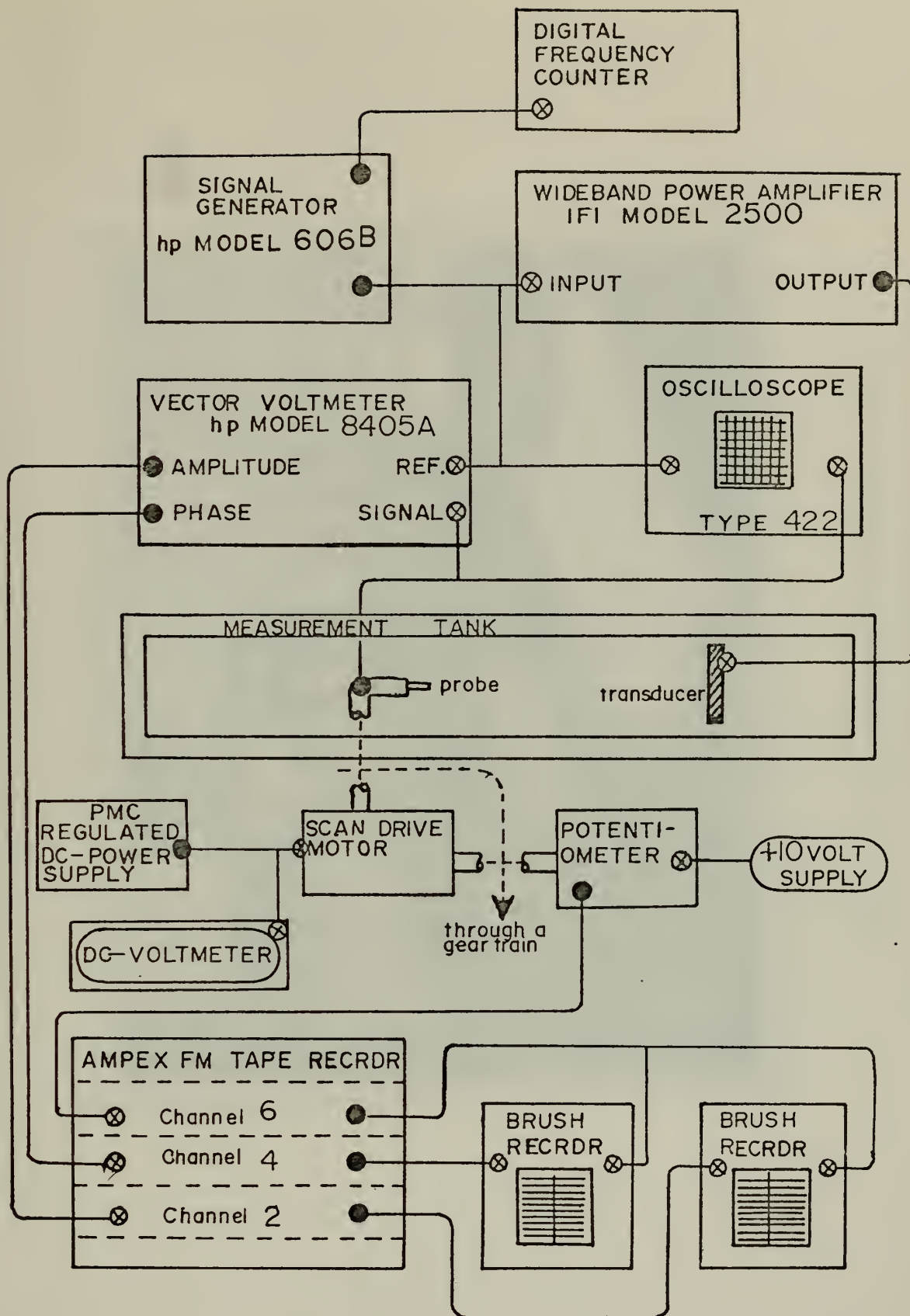
Figure 3-4. Electronic Equipment Layout.
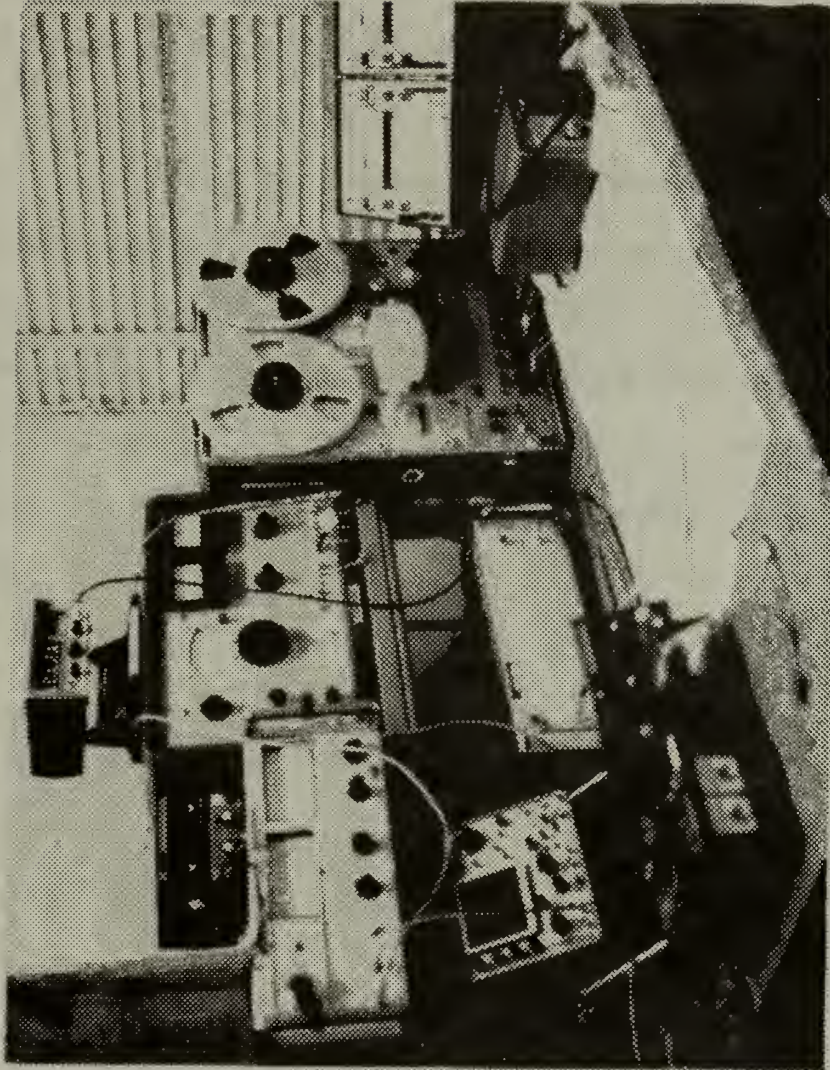
Figure 3-5. Electronic Equipment Setup.

G.   TYPICAL EXPERIMENTAL RESULTS

Figure 3-6 shows six typical records as recorded at successive depths by the analog type scanning equipment. Amplitude, phase, and potentiometer outputs are recorded simultaneously on separate channels. The experiment was designed to generate data for a 64 by 64 sample lattice, so the potentiometer output has a spike corresponding to each of 64 equally spaced positions of the hydrophone along the width of the record. This channel was used in the A/D conversion to trigger the sample circuit. Figure 3-7 shows the analog playback of the sampled data as recorded on magnetic tape after the A/D conversion. Comparison of the measured record and the converted record shows good agreement.
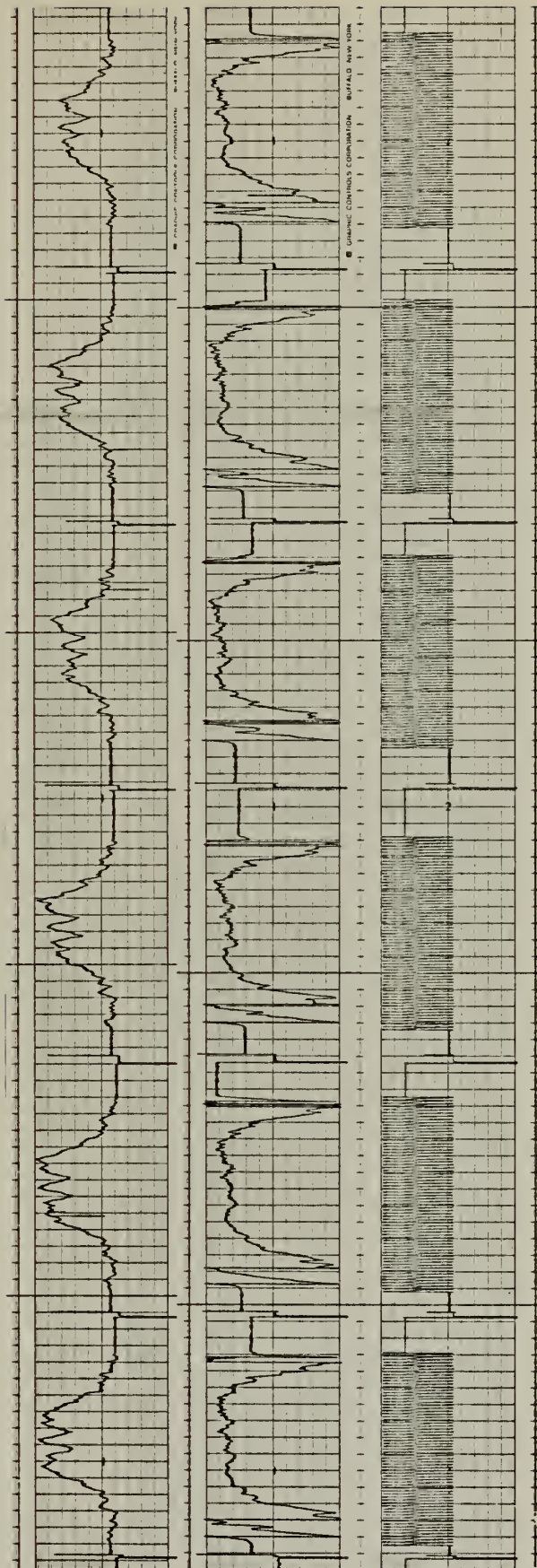
Figure 3-6. Six Typical Records of Amplitude, Phase, and Potentiometer Output (reading top to bottom) as Recorded at Successive Depths by the Scanning Equipment.

31
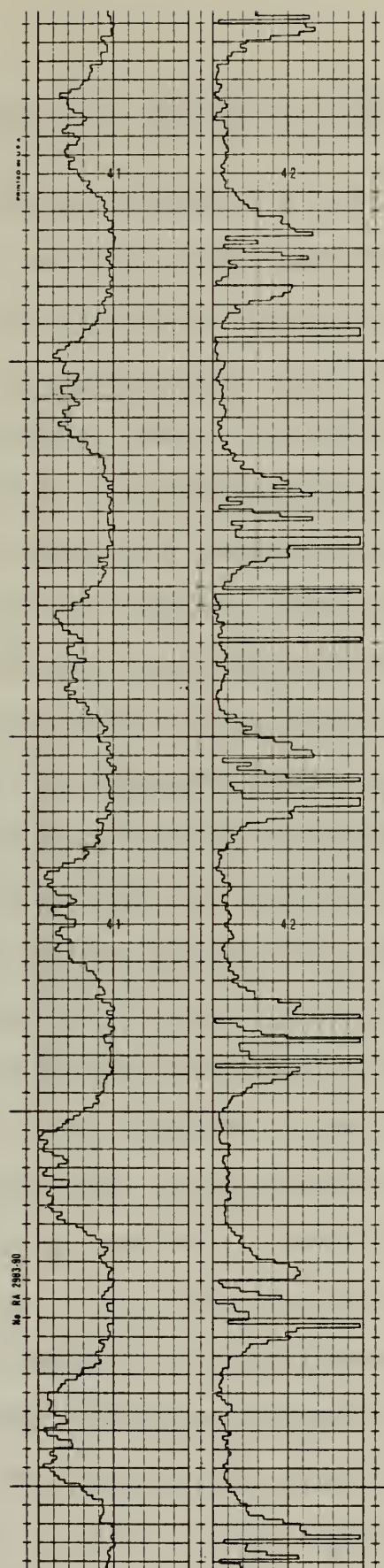
Figure 3-7. Six Typical Records of the Sampled Data Records Showing Amplitude and Phase (reading top to bottom) as Played Back from a Magnetic Tape in Analog Presentation.

32

IV. EXPERIMENTAL vs THEORETICAL RESULTS

A test of the computer program was the generation of a
far-field diffraction pattern. This was done by using a
small aperture whose diffraction pattern could be considered
to be in the far-field at distances well within the near-
field of the sample lattice used. The effect of the sample
lattice was introduced in the preceding section in the
discussion of the DFT where the scheme of making the aperture
to be modeled much smaller than the "data window" was pro-
posed. This scheme allows increased latitude in the range
of z for which the diffraction model can be considered valid.
If a sufficient number of discrete samples are taken to
accurately represent a square aperture, and a large border
of zeroed data is left around the aperture, then the window
does not disturb the desired diffraction pattern. It was
convenient to consider this effect in the following light:

The very-near-field of an aperture is essentially a
parallel projection of the aperture. The diffraction of a
small aperture diverges very rapidly and the far-field is
reached rather quickly in moving in the z-direction. The
diffraction pattern of a large aperture diverges more slowly
and the far-field is reached at much greater distances of
propagation. (The same radiation frequency for both aper-
tures is assumed.) The terminology "near-field of the data
window" will be used to refer to the region in which the

33

modeled aperture is valid. (Equation 2.9 which is the exact
and continuous form of the propagation model has no such
limitation on the region of the z axis in which it is valid.
The limitation is a result of a finite sample lattice and
with a large enough sample space the diffraction of any
aperture can be projected into the far-field with this
model.)

W. K. Pratt and H. C. Andrews [Ref. 20] have generated
computer far-field diffraction patterns which were used for
comparison to test the computer program for this work.
Figure 4-1 shows a typical diffraction pattern of a single
square aperture. The amplitude variations of the field
(ranging from 0.0 to 3.1 units) are present in five contour
levels, for a plane 96 wavelengths (96λ) from the aperture.
The divisions between levels are 0.7 units apart. The
width of the aperture, a, was 6λ and the width of the data
field was 38λ across. The pattern shown was as expected
from the analytic solution for a square aperture [Ref. 5].
A variety of criteria are found in the literature for deter-
mining the transition from the near-field to the far-field
region. According to Goodman [Ref. 5], this transition can
be given as

$$z \gg \frac{k(x^2+y^2)_{max}}{2} \qquad (4.1)$$

where z and k are as previously defined and x and y are
measured from the center of the aperture as shown in figs.
2.2 and 2.3. Writing Eq. 4.1 in terms of sampled data for
a square lattice gives the criterion

34
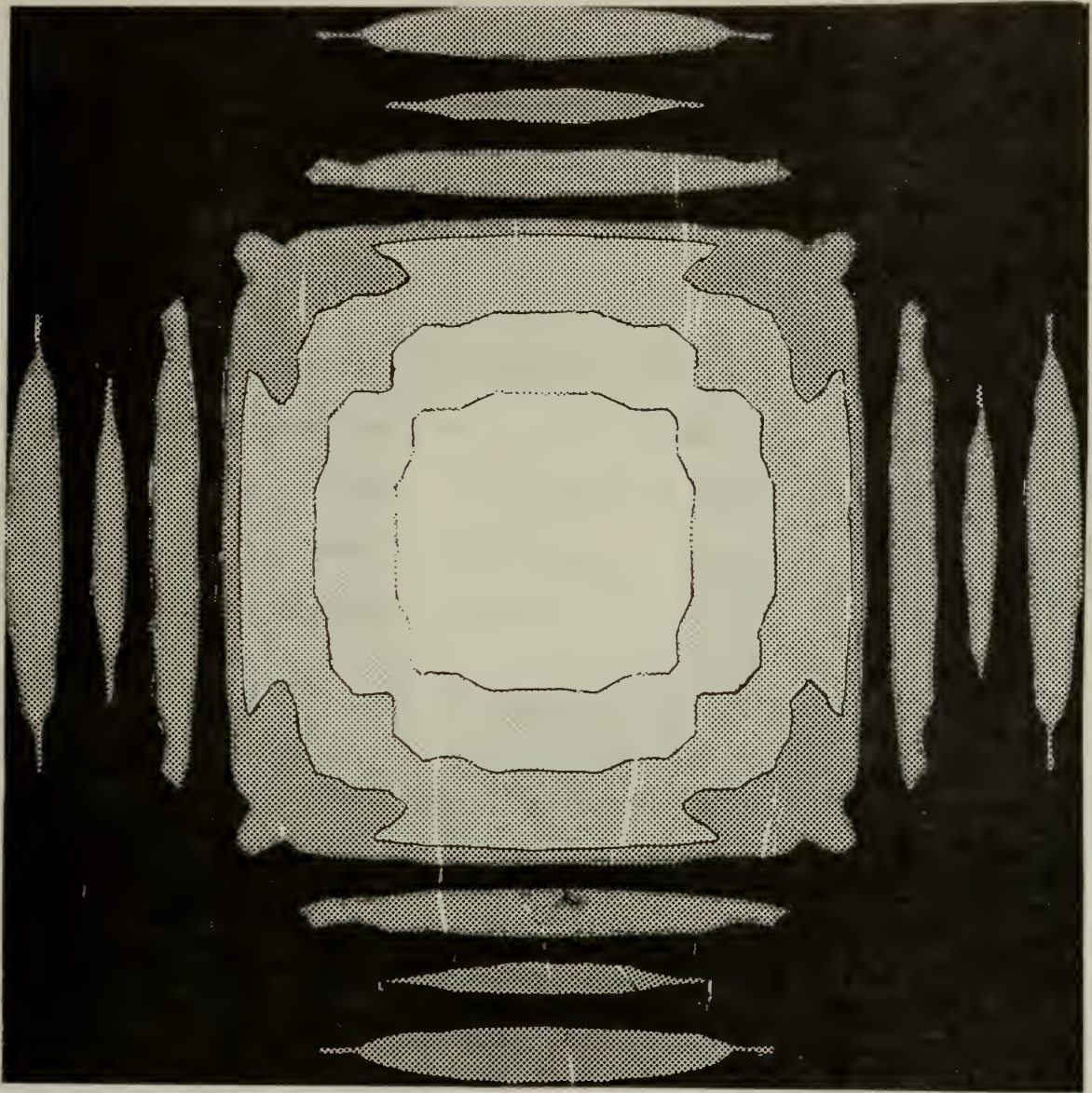
Figure 4-1.   Far-field Diffraction Pattern (amplitude) of a
              Square Aperture.   a/λ = 6, z = 96λ.

$$z \gg \frac{5\pi}{12} N^2 \lambda \qquad\qquad (4.2)$$

From this equation the maximum z for which the window does not appreciably interfere with the observed diffraction pattern is taken as

$$z_{max} = \frac{5\pi}{12} N^2 \lambda \qquad\qquad (4.3)$$

For example, the pattern shown in Fig. 4.1 is a square lattice of 32 samples giving a far-field for the data window beginning at $z \simeq 1340\lambda$. Applying the same equation (Eq. 4.1) to the maximum x and y, where $x_{max} = y_{max} = N/16$, the far-field of the aperture is where

$$z \gg \frac{2\pi}{\lambda} (\frac{N}{16} X)^2 \qquad \text{or} \qquad z \gg 17.4\lambda$$

It was expected, therefore, that Fig. 4-1 would be a reasonably accurate presentation of the far-field pattern of a square aperture out to $z \simeq 1340\lambda$.

In the preceding discussion the word aperture was used instead of the word transducer because of the type of distribution assumed at the transducer plane. When the following assumptions are made the transducer diffraction pattern is based entirely on its aperture function:

1. The motion of the transducer has uniform amplitude over its entire face.

2. The motion of the transducer is in phase over the entire face.

3. The motion of the medium immediately adjacent to the face of the transducer has the same motion as the transducer itself.

36

4. The medium outside of the edges of the transducer does not move due to the motion of the transducer.

The program was tested by its generation of aperture diffraction patterns. The ability to predict transducer diffraction patterns on the basis of an aperture diffraction pattern will be discussed in light of the experimental data.

The transducer shown in Fig. 3-1b was modeled on the IBM 360 computer and the field at $z = 73\lambda$ was predicted based upon its square aperture function. Figures 4-2 and 4-3 are the predictions of amplitude and phase respectively. Note that the transducer was a 2 inch square sheet of quartz, while the active face assumed in the model was a 1 3/4 inches square aperture. This was a correction for that portion of the transducer obscured by the mount. Additionally, the restriction in motion offered by the mount at the edges violates the assumption of uniform amplitude. This effect can be seen from the amplitude record made at 9.1λ in front of the transducer. Figure 4-4 shows a typical amplitude measurement at $z = 73\lambda$. The assumed shape at the transducer is shown by the heavy dotted line superimposed over the data record. Figures 4-5 and 4-6 are contour plots of the sampled data at $z = 9.1\lambda$ as recorded after the A/D conversion. The disparities in the predicted and measured contour patterns is attributable to the following inaccuracies:

1. The wavefront and measurement planes were slightly misaligned as seen from the phase record of Fig. 3-3. In order for the fourfold symmetry of Figs. 4-2 and 4-3 to be

37

Figure 4-2. Predicted Near-field Diffraction Pattern
            (amplitude) of a Square Transducer.
            $a/\lambda = 30$, $z = 73\lambda$.
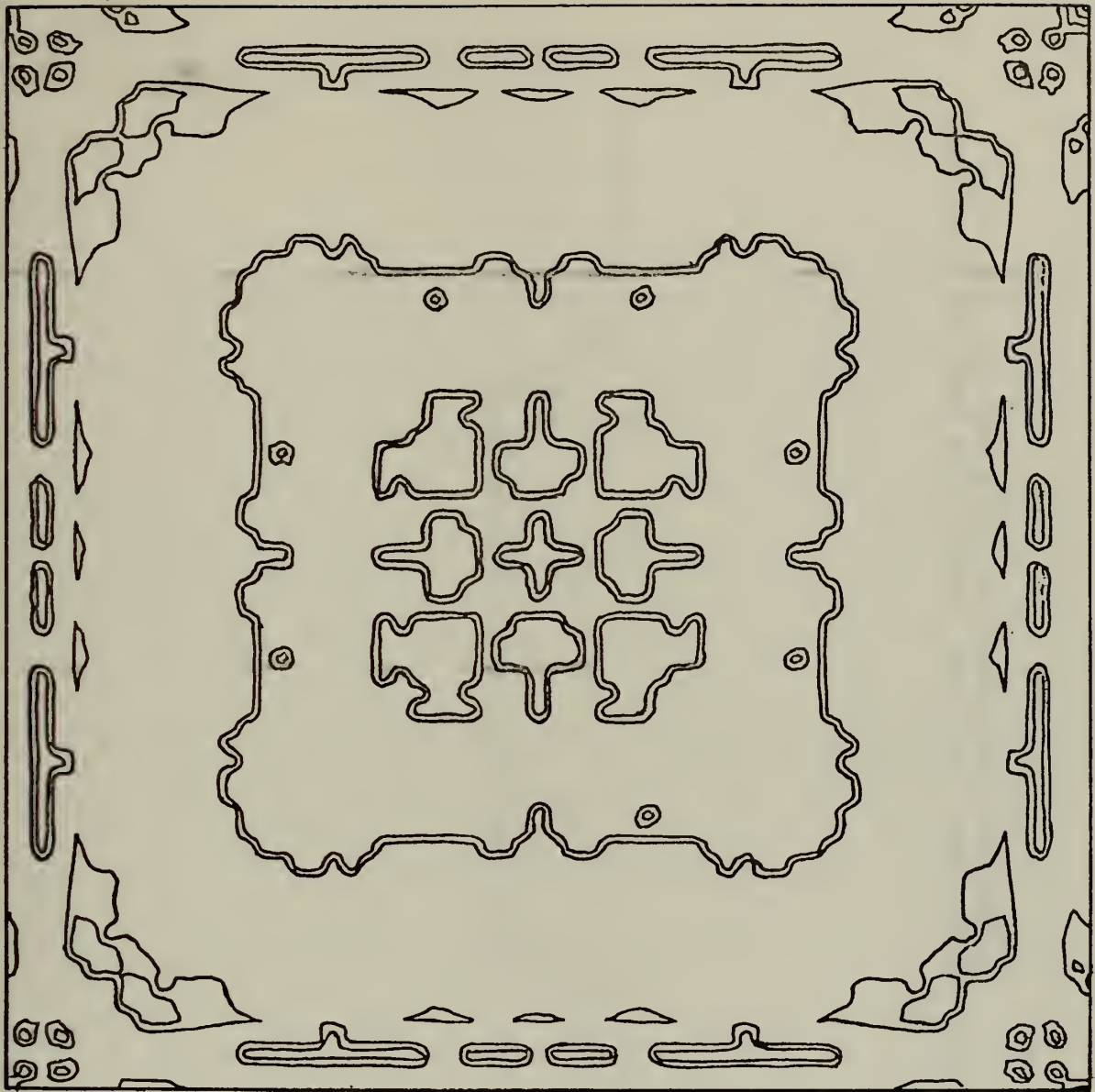
Figure 4-3.   Predicted Near-field Diffraction Pattern
              (phase) of a Square Transducer.
              $a/\lambda = 30$, $z = 73\lambda$.

Figure 4-4. Amplitude Variation Across the Face of a Quartz Transducer Radiating at 1012 kHz for $a/\lambda = 30$, at $z = 9.1\lambda$.
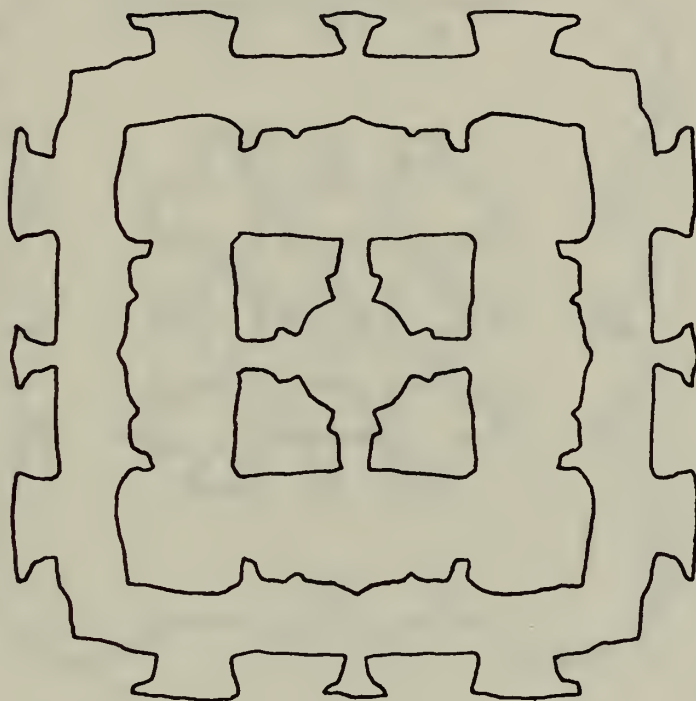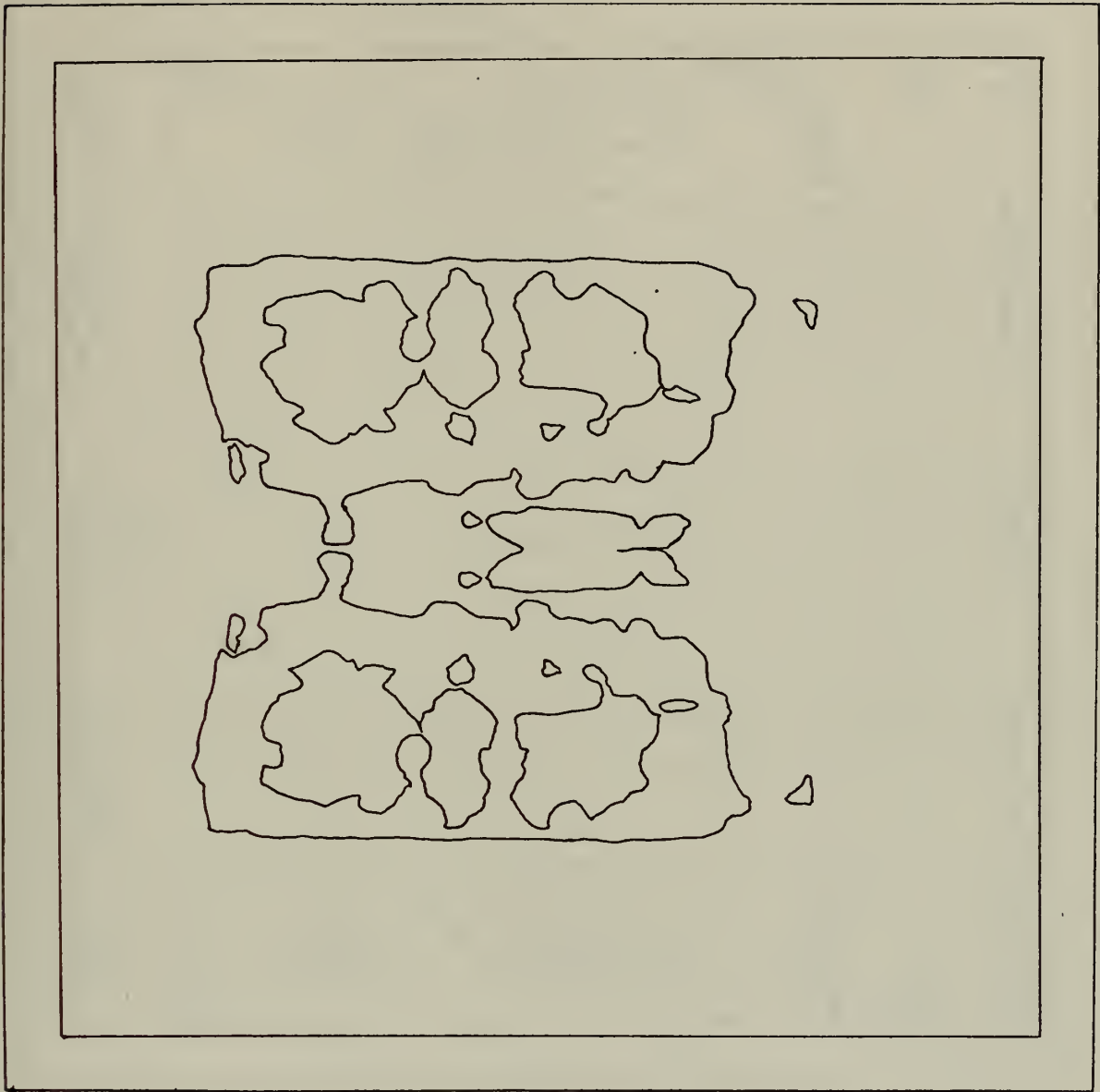
Figure 4-5. Measured Near-field Diffraction Pattern
(amplitude) of a Square Transducer $a/\lambda = 30$,
$z = 73\lambda$.

Figure 4-6. Measured Near-field Diffraction Pattern (phase)
of a Square Transducer $a/\lambda = 30$, $z = 73\lambda$.

present in the measured pattern the source must be aligned symmetrically with respect to the measurement plane. The misalignment also caused the propagating waveform to shift its center with respect to the center of the sample lattice.

2. Data were not taken of the entire plane. To conserve time in the recording and processing of data, only half of the plane was sampled; symmetry was assumed and the half-plane data was folded about a horizontal through the center. This gave a false symmetry to the data in view of the alignment difficulty.

3. Recording errors in the measurements taken were on the order of ±10 degrees for phase and ±4% for amplitude, due to inaccuracies of the recording equipment. The A/D conversion process introduced additional error, but no information was available on the accuracy of the program used other than the visual comparison from displays such as the one shown in Fig. 3-7.

4. Inaccuracies in the free-field assumption caused by the probe hydrophone, and by the boundaries in the tank were neglected.

5. Inaccuracies were inherent in evaluating a transducer's diffraction pattern based on its aperture function alone.

It is impossible to evaluate the validity of modeling the transducer by its aperture function on the basis of the comparisons presented here. If the data recorded at 9.1λ were propagated to the plane at 73λ and compared to the

measurements made there, the composite effect of the inaccu-
racies listed in (1) to (4) above could be determined. It
was concluded for the purpose of this experiment that the
aperture function model was sufficient for modeling small
transducers, and was found to be an adequate model when the
ratio of a/λ was less than 10.

Many acoustic imaging systems of interest require planar
ultrasonic fields at frequencies of 1 MHz and higher. An
array design approach to supplying this need was the motiva-
tion for developing the computer prediction capability. As
a preliminary study to the design problem a 3 x 3 array of
square transducers was chosen. After some experimenting with
the program it was found that at least 25 samples per trans-
ducer was required to produce an acceptable far-field
diffraction pattern for a square aperture. Each square
transducer was represented by an aperture 6 wavelengths on
a side. The spacing between these transducers had to be
wide enough so that interference between adjacent transducers
did not occur until a distance where the far-field pattern
of the individual transducers had already developed. This
effect is evident in the pattern shown in Fig. 4-7, where
the sound field can be described as a sum of nine spatially
separated far-field patterns. When the array was propagated
to greater and greater distances, the far-field patterns
expanded and merged together in a way which made the indi-
vidual far-field pattern distinguishable in the overall
field pattern. When the array was propagated to that distance
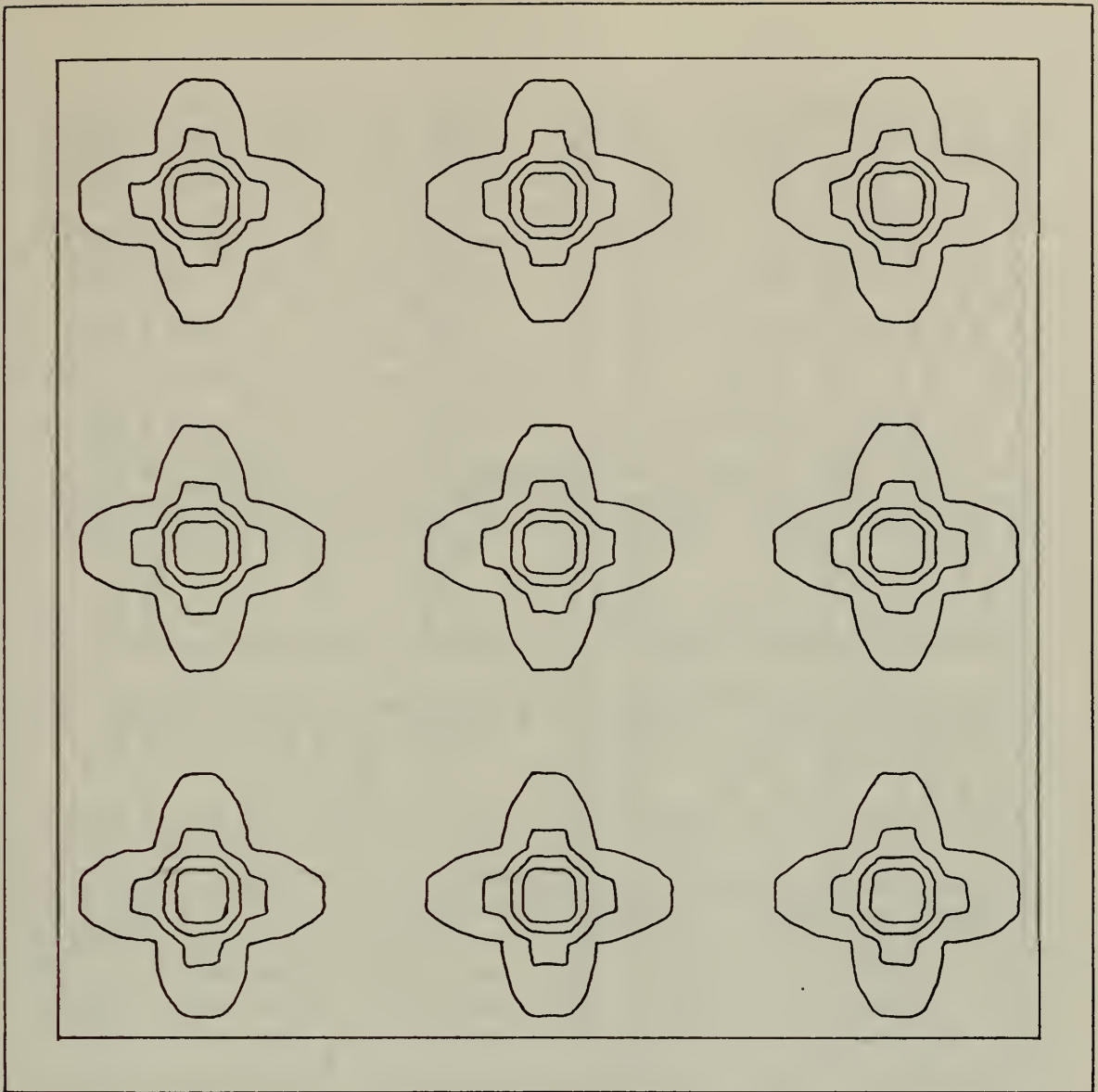
Figure 4-7. Diffraction Pattern for a transducer Array of 9 Uniformly Spaced Elements. The elements are squares,6 wavelengths on a side. The pattern is a prediction for a plane 60 wavelengths from the source plane. The contour levels are 2.8 units apart.

Figure 4-8. A Predicted Diffraction Pattern for a Transducer Array of 9 Uniformly Spaced Elements. The figure is one quadrant of a pattern which has four-fold symmetry. The elements are squares 6 wavelengths on a side. The pattern resents a plane 600 wavelengths from the source plane. The contour levels are 0.28 units apart.

where adjacent elements began to interfere, the field diffraction pattern became very complex and all similarity to the far-field pattern of a square was lost. Instead the pattern looked somewhat like the near-field diffraction pattern of a finely sampled square aperture. Figure 4-8 is an example of this effect which the author has called "the near-field diffraction of far-field sources". This nomenclature alludes to the fact that the individual transducers were in the far-field according to the criteria of Eq. 4.1 while the outer dimensions of the composite array placed the source as a whole in the near-field. This figure is the result of contouring only one quadrant and using a 128 x 128 sample lattice. (Note the symmetry of Fig. 4-8, and the improved resolution gained by the larger number of samples used.)

The use of the computer model appears to have much promise for designing an array to produce a desired waveform. There are a large number of variables which determine the form of the array diffraction. It was found, however, that the number of trials which must be run can be significantly narrowed by defining dimensionless quantities which model many different combinations of element size, element spacing and element shape. Variables which were not looked into in this preliminary study were the number of elements in the array, and the possible variations in driving the individual elements in various phase and amplitude combinations. If all feasible combinations of the variables mentioned were

to be examined for a design, it would be exhaustively time consuming and expensive. A major advantage of this approach is the intuitive feeling the user gains by running a few simple cases using well known aperture shapes. Familiarity with the geometry of some two-dimensional Fourier transforms [Ref. 21] coupled with a feeling for the general trends of propagation in the spatial frequency domain, would allow the designer to eliminate a large class of possible variables and to concentrate on those which have some intuitive promise. Facilities are available at the Naval Postgraduate School for immediate graphical response to a change in variables using the graphics display terminal which presents data on a rectangular cathode-ray tube. This type of data presentation used with a routine similar to the CONTUR subroutine would make the large number of variables involved manageable. The IBM/360 version of the propagation program as presented in Appendix B requires 250K core storage with the CONTUR subroutine included. This version requires approximately 56 seconds of model 67 cpu time to compile and calculate the data for the first projection of a square matrix of 64 x 64 samples. Each additional propagation of the data to another plane takes approximately 20 seconds. The time-memory requirement of the program appears to be adaptable to use with the graphic display units.

V. <u>CONCLUSIONS</u>

A recently developed technique for imaging by reproduction from object diffraction patterns has been applied to analyzing the sound source itself. The technique is not limited to ultrasound, but high frequency imaging applications were of particular interest for this study. Consequently, the experimental measurements were conducted at 1 MHz. Although most of the concepts and arguments can be applied to frequencies well below 1MHz, such applications were not considered herein.

A technique of computer modeling of the diffraction equations has been emphasized. The capability of the computer facilities at the Naval Postgraduate School to perform such diffraction calculations in a fast concise format has been accented.

The use of this technique in designing an array was a driving incentive in the work reported, and from the results of the preliminary array model examined it appears to be a worthwhile approach to production of a planar field of ultrasound.

The experimental portion of this work produced data for an elementary comparison with a computer prediction. The data has many applications for future work to give information about the transducer used, about the capability of the computer program, and about imaging system capabilities.

APPENDIX A

PROPAGATION PROGRAM - IBM 360/67 COMPUTER

THIS PROGRAM MODELS PROPAGATION OF AN ULTRASONIC SOUND
SOURCE AND PERFORMS PLANE-TO-PLANE PROJECTIONS OF A TWO-
DIMENSIONAL COMPLEX PRESSURE DISTRIBUTION. THE REFERENCE
PLANE DATA IS ENTERED INTO TWO REAL ARRAYS OF 64 X 64
SAMPLES GIVING A TOTAL RECORD LENGTH OF 4096 POINTS. THE
TWO REAL ARRAYS ARE USED TO FORM ONE COMPLEX ARRAY. THE
COMPLEX ARRAY IS TRANSFORMED TO THE SPATIAL FREQUENCY
PLANE USING THE SUBROUTINE FOUR2. PROPAGATION TO ANOTHER
PLANE IS PERFORMED BY A TRANSFER FUNCTION ALGORITHM WHICH
IS A MULTIPLIER IN THE TRANSFORMATION DOMAIN. THE INVERSE
TRANSFORM IS TAKEN USING THE SUBROUTINE FOUR2 AND THE DATA
AT THE NEW PLANE IS DISPLAYED ON THE PAGE PRINTER AND ON
THE CALCOMP PLOTTER BY USE OF THE SUBROUTINE CONTUR.
        THIS IS ONE OF THREE BASIC PROGRAMS WRITTEN TO OPTIMIZE
THE TIME-MEMORY TRADE-OFF FOR A PARTICULAR TRANSDUCER TYPE.
SEE.....'A COMPUTER TECHNIQUE FOR NEAR-FIELD ANALYSIS OF AN
ULTRASONIC TRANSDUCER',GRIGGS,C.A.,M.S. THESIS, U.S. NAVAL
POSTGRADUATE SCHOOL, CALIFORNIA,MONTEREY,1973

```
      IMPLICIT COMPLEX*8(D)
      REAL*8 TITLE(12)
      REAL*8 LABEL(12)
```

DISTANCES TO BE LABELED ON CONTOUR PLOTS ARE ENTERED HERE

```
      REAL*8 ZTITLE(1)/'  O X   '/
      LOGICAL*1 LTG(3)
      DIMENSION CLM(4),CLP(4)
      DIMENSION DATA(64,64),NN(2),DATAVC(4096), AMAGVC(4096)
     1PHAVC(4096),XVEC(64),YVEC(64),YVECP(64)
      COMMON/AREA1/AMAG(64,64),PHA(64,64)
      DIMENSION DCOPY(64,64),DCOPVC(4096)
      EQUIVALENCE (DATA(1,1),DATAVC(1)),(AMAG(1,1),AMAGVC(1)
      EQUIVALENCE (PHA(1,1),PHAVC(1))
C
C     INITIAL VALUES OF N AND M
      DATA NN/64,64/
```

LABELS WHICH APPEAR ON THE CONTOUR DRAWINGS ARE ENTERED
HERE WITH DISTANCES DEPENDENT UPON DATA ABOVE AND NOT ON
THE ACTUAL VALUE OF 'Z' IN THE PROGRAM

```
      DATA TITLE/'        ',
     1           '       A',
     2           'MPLITUDE',
     3           ' CONTOUR',
     4           '        ',
     5           '        ',
     5           'ONE SQ T',
     6           'RANSDUCE',
     7           'R     Z=',
     C           '        ',
     C           '       C',
     C           'A GRIGGS'/
      DATA LABEL/'        ',
     1           '        ',
     2           '   PHASE',
     3           ' CONTOUR',
     4           '        ',
     5           '        ',
     5           'ONE SQ T',
     6           'RANSDUCE',
     7           'R     Z=',
     C           '        ',
     C           '       C',
     C           'A GRIGGS'/
```

50

```
          LTG(1)=.TRUE.
          LTG(2)=.FALSE.
          LTG(3)=.FALSE.
          NINT=NN(1)
          MINT=NN(2)
          NREL=(NINT+2)/2
          MREL=(MINT+2)/2
          REALN=FLOAT(NINT)
          REALM=FLOAT(MINT)
          NDIM=NN(1)
          MDIM=NN(2)
          NVEC=NDIM*MDIM
          B=0.0
          PI=3.14159265
          DJ=(0.0,1.0)
          DO 999 K=1,NVEC
          DATAVC(K)=(0.0,0.0)
          AMAGVC(K)=(0.0)
          PHAVC(K)=(0.0)
          DCOPVC(K)=(0.0)
      999 CONTINUE
C
C     READING MEASURED DATA
C
```

AS AN OPTIONAL METHOD OF ENTERING DATA SIMULATED DATA CAN
BE GENERATED AND ENTERED DIRECTLY INTO THE COMPLEX ARRAY.

```
          READ (5,100) (AMAGVC(K),K=1,2048)
          READ(5,100) (PHAVC(K),K=1,2048)
      100 FORMAT(5(F9.4,5X))
C
C     READING DATA INTO DATA(I,J)
C
          DO 1001 J=1,29
          DO 1001 I=1,64
          PEAK=(AMAG(I,J)+8.0)/9.6
          PHI=PHA(I,J)*(PI/99.0)
          CLIP=J+3
          DATA(I,CLIP)=CMPLX(PEAK,PHI)
     1001 DCOPY(I,CLIP)=DATA(I,CLIP)
C
C     CNE RECORD TAKEN OUT OF ORDER
C
```

THIS PARTICULAR VERSION PERFORMED SOME CORRECTIONS TO THE
DATA BECAUSE OF THE DATA RECORDING PROCESS. TWO ROWS IN
THE MATRIX WERE INTERCHANGED AND THE DATA WAS SHIFTED TO
CORRECT FOR THE POINT OF SYMMETRY. IT ALSO FOLDS A HALF
PLANE OF CATA ASSUMING TWO-FOLD SYMMETRY.

```
          J=28
          DO 1002 I=1, 64
          ORDER=J+1
          DATA(I,J)=DCOPY(I,ORDER)
     1002 CATA(I,ORDER)=DCOPY(I,J)
          DO 1003 J=33,64
          DO 1003 I=1,64
          FOLD=65-J
     1003 CATA(I,J)=DATA(I,FOLD)
          CALL CONVRT(DATAVC,AMAGVC,PHAVC)
C
          WRITE(6,3130)
     3130 FORMAT('1',T57,'INPUT ARRAY'/)
          CALL OUTPUT
C
```

SINCE THE DISCRETE TRANSFORM IS INDEXED FROM ZERO TO N MINUS
ONE THE TRANSFORM IS CENTERED ABOUT A POINT SHIFTED BY
N DIVIDED BY TWO SAMPLES TO THE RIGHT AND UP IN THE FIRST
QUADRANT THE INPUT DATA MUST BE SHIFTED ALSO TO MATCH
THIS AMOUNTS TO A PHASE SHIFT IN THE SPATIAL FREQUENCY PLANE

```
      DO 2001 I=1,NDIM
      DO 2001 J=1,MDIM
      DEX=(DJ*PI*(I+J))
      DSHIF=CEXP(DEX)
      DATA(I,J)=DATA(I,J)*DSHIF
 2001 CONTINUE
C
      CALL FOUR2(DATA,NN,2,-1)
C
C     DATA(I,J) ARE NOW THE FOURIER COEFFICIENTS (SHIFTED)
C
      DO 2002 KOPY=1,NVEC
 2002 DCOPVC(KOPY)=DATAVC(KOPY)
      Z=0.0
      LOOP=1
      ALAM=1.08853774
      DO 2003 KAT=1,NVEC
 2003 DATAVC(KAT)=DCOPVC(KAT)




C    PROPAGATION BY SPATIAL FREQUENCY TRANSFER FUNCTION.


      WAVE=1.0/(ALAM*ALAM)
      FREQX=1.0/REALN
      FREQY=1.0/REALM
      DO 3003 K=1,NDIM
      KINT=K-(NINT+2)/2
      PRIMEK=FLOAT(KINT)
      FXK=FREQX*PRIMEK
      FXKSQ=FXK*FXK
      DO 3003 L=1,MDIM
      LINT=L-(MINT+2)/2
      PRIMEL=FLOAT(LINT)
      FYL=FREQY*PRIMEL
      FYLSQ=FYL*FYL
      EVANS=(WAVE-FXKSQ-FYLSQ)
 3000 RADIAN=2.0*PI
      ROOT=SQRT(EVANS)
      DPROP=DJ*RADIAN*Z*ROOT
      DTRANS=CEXP(DPROP)
      DATA(K,L)=DATA(K,L)*DTRANS
      GO TO 3002
 3001 DATA(K,L)=(0.0,0.0)
 3002 CONTINUE
 3003 CONTINUE




      CALL FOUR2 (DATA,NN,2,1)

      DO 6004 I=1,NDIM
      DO 6004 J=1,MDIM
      PDIM=1.0/(REALN*REALM)
      DIMPLX=CMPLX(PDIM,B)
      DEX=(-CJ*PI*(I+J))
      DSHIF=CEXP(DEX)
      DATA(I,J)=DATA(I,J)*DIMPLX*DSHIF
 6004 CONTINUE
      CALL CONVRT(DATAVC,AMAGVC,PHAVC)
      WRITE(6,6005) Z,REF
```

52

```
6005 FORMAT ('1',T57,'INPUT ARRAY PROPAGATED TO Z=',F5.1/
    2'0',T57,'PHASE REFERENCE =',F5.1,'   DEGREES'/)
      CALL OUTPUT

C     REFERENCE PHASE TO UNDIFFRACTED RAY IN DEGREES

      DO 6009 K=1, NVEC
      PHAVC(K)=(PHAVC(K)*(180.0/PI))+180.0
      REF=PHA(NREL,MREL)
      PHAVC(K)=ABS(PHAVC(K)-REF)
      IF(PHAVC(K).LE.180.0) GO TO 6009
      PHAVC(K)=360.0-PHAVC(K)
 6009 CONTINUE
      TITLE(10)=ZTITLE(LOOP)
      LABEL(10)=ZTITLE(LOOP)
      CALL CONTUR (AMAG,64,64,64,CLM,-4,TITLE,9,9,LTG)
      CALL CONTUR (PHA,64,64,64,CLP,-4,LABEL,9,9,LTG)
      Z=Z+20.0
      STOP
      END




      SUBROUTINE CONVRT(DATAVC,AMAGVC,PHAVC)
      IMPLICIT COMPLEX*8 (D)
      DIMENSION DATAVC(4096),AMAGVC(4096),PHAVC(4096)
      DO 1080 K=1,4096
      REALP=REAL(DATAVC(K))
      AIMAGP=AIMAG(DATAVC(K))
      AMAGVC(K)=SQRT(REALP**2+AIMAGP**2)
      TRY=AMAGVC(K)
      IF(TRY.EQ.0.0) GO TO 1070
      PHAVC(K)=ATAN2(AIMAGP,REALP)
      GO TO 1080
 1070 PHAVC(K)=0.0
 1080 CONTINUE
      RETURN
      END




C SUBROUTINE OUTPUT FOR A 64 X 64


      SUBROUTINE OUTPUT
      COMMON/AREA1/AMAG(64,64),PHA(64,64)
      WRITE(6,3031) (J,J=33,64)
 3031 FORMAT('0',4X,32I4)
      DO 3040 I=33,64
      WRITE(6,3032)(I,(AMAG(I,J),J=33,64))
 3032 FORMAT('0',I3,1X,32F4.1)
      WRITE(6,3033)(PHA(I,J),J=33,64)
 3033 FORMAT('0',4X,32F4.1/)
 3040 CONTINUE
      RETURN
      END
```

```
      SUBROUTINE FOUR2(DATA,NN,NDIM,ISIGN)
      DIMENSION DATA(1),NN(1)
      IF(NDIM-1)700,1,1
    1 NTOT=2
      DO 2 IDIM=1,NDIM
      IF(NN(IDIM))700,700,2
    2 NTOT=NTOT*NN(IDIM)
      TWOPI=6.2831853070
      RTHLF=.7071067812
      NP1=2
      DO 600 IDIM=1,NDIM
      N=NN(IDIM)
      NP2=NP1*N
      IF(N-1)700,600,100
  100 NP2HF=NP2/2
      J=1
      DO 160 I2=1,NP2,NP1
      IF(J-I2)110,130,130
  110 I1MAX=I2+NP1-2
      DO 120 I1=I2,I1MAX,2
      DO 120 I3=I1,NTOT,NP2
      J3=J+I3-I2
      TEMPR=DATA(I3)
      TEMPI=DATA(I3+1)
      DATA(I3)=DATA(J3)
      DATA(I3+1)=DATA(J3+1)
      DATA(J3)=TEMPR
  120 DATA(J3+1)=TEMPI
  130 M=NP2HF
  140 IF(J-M)160,160,150
  150 J=J-M
      M=M/2
      IF(M-NP1)160,140,140
  160 J=J+M
      NP1TW=NP1+NP1
      IPAR=N
  310 IF(IPAR-2)350,330,320
  320 IPAR=IPAR/4
      GO TO 310
  330 DO 340 I1=1,NP1,2
      DO 340 K1=I1,NTOT,NP1TW
      K2=K1+NP1
      TEMPR=DATA(K2)
      TEMPI=DATA(K2+1)
      DATA(K2)=DATA(K1)-TEMPR
      DATA(K2+1)=DATA(K1+1)-TEMPI
      DATA(K1)=DATA(K1)+TEMPR
  340 DATA(K1+1)=DATA(K1+1)+TEMPI
  350 MMAX=NP1
  360 IF(MMAX-NP2HF)370,600,600
  370 LMAX=MAXO(NP1TW,MMAX/2)
      DO 570 L=NP1,LMAX,NP1TW
      M=L
      IF(MMAX-NP1)420,420,380
  380 THETA=-TWOPI*FLOAT(M)/FLOAT(4*MMAX)
      IF (ISIGN)400,390,390
  390 THETA=-THETA
  400 WR=COS(THETA)
      WI=SIN(THETA)
  410 W2R=WR*WR-WI*WI
      W2I=2.0*WR*WI
      W3R=W2R*WR-W2I*WI
      W3I=W2R*WI+W2I*WR
  420 DO 530 I1=1,NP1,2
      KMIN=IPAR*M+I1
```

```
      IF(MMAX-NP1)430,430,440
430   KMIN=I1
440   KDIF=IPAR*MMAX
450   KSTEP=4*KDIF
      DO 520 K1=KMIN,NTOT,KSTEP
      K2=K1+KDIF
      K3=K2+KDIF
      K4=K3+KDIF
      IF(MMAX-NP1)460,460,480
460   U1R=DATA(K1)+DATA(K2)
      U1I=DATA(K1+1)+DATA(K2+1)
      U2R=DATA(K3)+DATA(K4)
      U2I=DATA(K3+1)+DATA(K4+1)
      U3R=DATA(K1)-DATA(K2)
      U3I=DATA(K1+1)-DATA(K2+1)
      IF(ISIGN)470,475,475
470   U4R=DATA(K3+1)-DATA(K4+1)
      U4I=DATA(K4)-DATA(K3)
      GO TO 510
475   U4R=DATA(K4+1)-DATA(K3+1)
      U4I=DATA(K3)-DATA(K4)
      GO TO 510
480   T2R=W2R*DATA(K2)-W2I*DATA(K2+1)
      T2I=W2R*DATA(K2+1)+W2I*DATA(K2)
      T3R=WR*DATA(K3)-WI*DATA(K3+1)
      T3I=WR*DATA(K3+1)+WI*DATA(K3)
      T4R=W3R*DATA(K4)-W3I*DATA(K4+1)
      T4I=W3R*DATA(K4+1)+W3I*DATA(K4)
      U1R=DATA(K1)+T2R
      U1I=DATA(K1+1)+T2I
      U2R=T3R+T4R
      U2I=T3I+T4I
      U3R=DATA(K1)-T2R
      U3I=DATA(K1+1)-T2I
      IF(ISIGN)490,500,500
490   U4R=T3I-T4I
      U4I=T4R-T3R
      GO TO 510
500   U4R=T4I-T3I
      U4I=T3R-T4R
510   DATA(K1)=U1R+U2R
      DATA(K1+1)=U1I+U2I
      DATA(K2)=U3R+U4R
      DATA(K2+1)=U3I+U4I
      DATA(K3)=U1R-U2R
      DATA(K3+1)=U1I-U2I
      DATA(K4)=U3R-U4R
520   DATA(K4+1)=U3I-U4I
      KMIN=4*(KMIN-I1)+I1
      KDIF=KSTEP
      IF(KDIF-NP2HF)450,450,530
530   CONTINUE
      M=M+LMAX
      IF(M-MMAX)540,540,570
540   IF(ISIGN)550,560,560
550   TEMPR=WR
      WR=(WR+WI)*RTHLF
      WI=(WI-TEMPR)*RTHLF
      GO TO 410
560   TEMPR=WR
      WR=(WR-WI)*RTHLF
      WI=(TEMPR+WI)*RTHLF
      GO TO 410
570   CONTINUE
      IPAR=3-IPAR
      MMAX=MMAX+MMAX
      GO TO 360
600   NP1=NP2
700   RETURN
      END
```

GENERAL DESCRIPTION AND SPECIFICATION SUMMARY
OF MAJOR ELECTRONIC COMPONENTS

EQUIPMENT NAME	TAPE RECORDER	POWER AMPLIFIER	VECTOR VOLTMETER
MANUFACTURER	Ampex	Instruments for Industry	Hewlett Packard
MODEL NO.	SP-300	M-2500	8405A
GENERAL DESCRIPTION	Direct recorder and reproducer. 7 channel recorder Speeds: 1-7/8, 3-3/4, 7 1/2, & 15 ips. FM Record/Reproduce capabilities only are listed.	A broad band power amplifier designed for power requirements up to 5 watts over the frequency range 10 KHz to 220 MHz. It has a minimum power gain of 27 db	A voltmeter and phasemeter for measuring the amplitude and phase relationship of two R.F. voltages R.F. range is 1-1000 MHz. A D.C. recorder output has a proportional d.c. voltage output for amplitude and phase
INPUT / OUTPUT CHARACTERISTICS	Input level: 0.5 to 10 volts rms causes 100% modulation Input impedance: 10 K ohms Output impedance 100-ohms Frequency Response 0 to 312 Hz @ 1-7/8 ips.	Input for full rated output +10 dbm standard. Input impedance: 50 ohms Output impedance: 50 ohms Bandpass Ripple: ±1.5 db max.	Impedance: 0.1 Megohm input 10,000 ohms output Input: Voltage: Ch.A: 1.5 mV to 1 V rms Ch.B: 100 µV to 1 V rms Output: Amplitude: 0 to 1 V d.c. ±6% Phase: 0 to ±0.5 V d.c. ±6%

LIST OF REFERENCES

1. Powers, J. P., and Griggs, C., "Large-Area Ultrasonic Fields for Acoustic Imaging," <u>Ultrasonics Symposium Proceedings</u>, p. 104-108, October 1972.

2. McKinney, C. M., Harvel, K. W., and Ellis, G. E., "Characteristics of Line and Disk Underwater Sound Transducers in the Near-to Farfield Transition Region," <u>The Journal of the Acoustical Society of America</u>, v. 51, p. 1076-1081, 17 August 1971.

3. Boyer, A. L., and others, "Teconstruction of Ultrasonic Images by Backward Propagation," <u>Acoustical Holography</u>, v. 3, p. 333-348, 31 July 1970.

4. Ratcliffe, J. A., "Some Aspects of Diffraction Theory and Their Application to the Ionosphere," <u>Reports on Progress in Physics</u>, v. 19, The Physical Society, London, 1956.

5. Goodman, J. W., <u>Introduction to Fourier Optics</u>, p. 48-50, 62-65, McGraw-Hill, 1968.

6. Shewell, J. R., and Wolf, E., "Inverse Diffraction and a New Reciprocity Theorem," <u>Journal of the Optical Society of America</u>, v. 58, p. 1596-1603, December 1968.

7. Cooper, G. R., and McGilem, C. D., <u>Methods of Signal and System Analysis</u>, p. 11-12, Holt, Rinehart, and Winston, Inc., 1967.

8. Thomas, J. B., <u>An Introduction to Statistical Communication Theory</u>, p. 140-144, Wiley, 1969.

9. Brenner, N. M., "Three Fortran Programs that Perform the Cooley-Tukey Fourier Transform," <u>IEEE Transactions on Audio and Electroacoustics</u>, v. AU-17, No. 2, p. 93-103, June 1969.

10. Jones, R. D., <u>Time Series Analysis of Analog Data by Analog-to-Digital and Digital Processing Methods at the Naval Postgraduate School</u>, M.S. Thesis, Naval Postgraduate School, California, Monterey, 1971.

11. Naval Postgraduate School Technical Note No. 0211-03, <u>Plotting Package for NPGS IBM 360/67</u>, by P. C. Johnson, February 1969.

12. Cooley, J. W., and Tukey, J. W., "An Algorithm for the
     Machine Calculation of Complex Fourier Series,"
     Mathematics of Computers, v. 19, p. 297-301, April
     1965.

13. Sondhi, M. M., "Reconstruction of Objects from Their
     Sound-Diffraction Patterns," The Journal of the
     Acoustical Society of America, v. 46, no. 5,
     p. 1158-1164, 30 April 1969.

14. Bergland, G. D., "A Guided Tour of the Fast Fourier
     Transform," IEEE Spectrum, p. 41-52, July 1969.

15. Cochran, W. T. and others, "What is the Fast Fourier
     Transform?", p. 45-55, IEEE Transactions on Audio
     and Electroacoustics, v. AU-15, no. 2, June 1969.

16. Bertram, S., "Frequency Analysis Using Discrete Fourier
     Transform," IEEE Transactoins on Audio and Electro-
     acoustics, v. Au-18, no. 4, p. 495-500, December
     1970.

17. Peterson, D. P. and Middleton, D., Information Control,
     v. 5, p. 279-323, 1962.

18. Papoulis, A., Systems and Transforms with Applications
     in Optics, p. 119-132, McGraw-Hill, 1968.

19. Singleton, R. C., "An Algorithm for Computing the Mixed
     Radix Fast Fourier Transform," IEEE Transactions
     on Audio and Electroacoustics, v. AU-17, no. 2,
     p. 93-103, June 1969.

20. Pratt, W. K., and Andrews, H. C., "Computer Calculated
     Diffraction Patterns," Applied Optics, v. 7, no. 2,
     p. 378-379, February 1968.

21. Bracewell, R., The Fourier Transform and Its Applications,
     p. 246-247, McGraw-Hill, 1965.

INITIAL DISTRIBUTION LIST

No. Copies

1. Defense Documentation Center   2
    Cameron Station
    Alexandria, Virginia   22314

2. Library, Code 0212   2
    Naval Postgraduate School
    Monterey, California   93940

3. Asst. Professor J. P. Powers, Code 52 Po   1
    Department of Electrical Engineering
    Naval Postgraduate School
    Monterey, California   93940

4. Asst. Professor A. I. Eller, Code 61Er   1
    Department of Physics
    Naval Postgraduate School
    Monterey, California   93940

5. LCDR Carlton A. Griggs, USN   1
    USS WAHOO (SS 565)
    FPO San Francisco, California   96601

6. Asst. Professor V. M. Powers, Code 52Pw   1
    Department of Electrical Engineering
    Naval Postgraduate School
    Monterey, California   93940

DOCUMENT CONTROL DATA · R & D

(Security classification of title, body of abstract and indexing annotation must be entered when the overall report is classified)

1. ORIGINATING ACTIVITY *(Corporate author)*	2a. REPORT SECURITY CLASSIFICATION
Naval Postgraduate School Monterey, California 93940	Unclassified
	2b. GROUP

3. REPORT TITLE

A COMPUTER TECHNIQUE FOR NEAR-FIELD ANALYSIS
OF AN ULTRASONIC TRANSDUCER

4. DESCRIPTIVE NOTES *(Type of report and, inclusive dates)*

Master's Thesis; March, 1973

5. AUTHOR(S) *(First name, middle initial, last name)*

Carlton A. Griggs; Lieutenant Commander, United States Navy

6. REPORT DATE	7a. TOTAL NO. OF PAGES	7b. NO. OF REFS
March 1973	61	21

8a. CONTRACT OR GRANT NO.	9a. ORIGINATOR'S REPORT NUMBER(S)
b. PROJECT NO.	
c.	9b. OTHER REPORT NO(S) *(Any other numbers that may be assigned this report)*
d.	

10. DISTRIBUTION STATEMENT

Approved for public release; distribution unlimited.

11. SUPPLEMENTARY NOTES	12. SPONSORING MILITARY ACTIVITY
	Naval Postgraduate School Monterey, California 93940

13. ABSTRACT

A computer technique for obtaining near-field cross-section views of an ultrasonic field is presented. The technique is applied to ultrasonic transducer radiation patterns with sample contour drawings of several cross-sections. A spatial frequency spectrum formulation of diffraction theory is chosen for the computations which are performed with the aid of a fast Fourier transform routine.

By experimentation an actual ultrasonic field was generated using a quartz transducer and the field was measured in a cross-sectional plane. A computer generated drawing of the measured data is compared to the drawing of a computer generated prediction of the field at the same plane.

The computer model is applied to an array of transducers to investigate the resulting ultrasonic field, as a preliminary use of the technique for array design.

DD FORM 1473 (PAGE 1)
1 NOV 65

S/N 0101-807-6811

UNCLASSIFIED
Security Classification

A-31408

14 KEY WORDS	LINK A		LINK B		LINK C	
	ROLE	WT	ROLE	WT	ROLE	WT
ULTRASONICS						
ACOUSTIC IMAGING						
TRANSDUCER DESIGN						
COMPUTER DIFFRACTION CALCULATION						